

Articles

A New Series of Highly Potent Non-Peptide Bradykinin B₂ Receptor Antagonists Incorporating the 4-Heteroarylquinoline Framework. Improvement of Aqueous Solubility and New Insights into Species Difference

Yuki Sawada,[†] Hiroshi Kayakiri,^{*,‡} Yoshito Abe,[†] Keisuke Imai,[§] Tsuyoshi Mizutani,[†] Noriaki Inamura,[‡] Masayuki Asano,[#] Ichiro Aramori,[#] Chie Hatori, Akira Katayama, Teruo Oku, and Hirokazu Tanaka[†]

Exploratory Research Laboratories, Fujisawa Pharmaceutical Co. Ltd., 5-2-3 Tokodai, Tsukuba, Ibaraki 300-2698, Japan

Received April 8, 2003

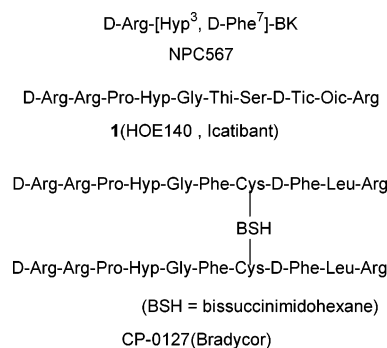
Introduction of nitrogen-containing heteroaromatic groups at the 4-position of the quinoline moiety of our non-peptide B₂ receptor antagonists resulted in enhancing binding affinities for the human B₂ receptor and reducing binding affinities for the guinea pig one, providing new structural insights into species difference. A CoMFA study focused on the diversity of the quinoline moiety afforded correlative and predictive QSAR models of binding for the human B₂ receptor but not for the guinea pig one. A series of 4-(1-imidazolyl)quinoline derivatives could be dissolved in a 5% aqueous solution of citric acid up to a concentration of 10 mg/mL. A representative compound **48a** inhibited the specific binding of [³H]BK to the cloned human B₂ receptor expressed in Chinese hamster ovary cells with an IC₅₀ value of 0.26 nM and significantly inhibited BK-induced bronchoconstriction in guinea pigs even at 1 μg/kg by intravenous administration.

Introduction

Human kinins consist of two endogenous peptides, bradykinin (BK; Arg¹-Pro²-Pro³-Gly⁴-Phe⁵-Ser⁶-Pro⁷-Phe⁸-Arg⁹) and kallidin (KD; [Lys⁰]BK; Lys¹-Arg²-Pro³-Pro⁴-Gly⁵-Phe⁶-Ser⁷-Pro⁸-Phe⁹-Arg¹⁰). BK is generated from high molecular weight kininogen by plasma kallikrein, while kallidin is released by tissue kallikrein from low molecular weight kininogen and is successively converted to BK through the action of aminopeptidases. Kinins can be degraded by a variety of enzymes called kininases, including kininase I, which cleaves the C-terminal arginine from kinins to produce [des-Arg⁹]BK and [des-Arg¹⁰]KD.¹

There are at least two subtypes of specific G-protein-coupled cell surface receptors, designated as B₁ and B₂, both of which have been identified by molecular cloning and pharmacological means.^{2–4} C-Terminal des-arginated derivatives of kinins have strong affinities for the B₁ receptor, which is induced under stressful and inflammatory conditions.^{5–7} On the other hand, kinins

Chart 1. Representative Peptide B₂ Receptor Antagonists



are highly potent agonists of the B₂ receptor, which is expressed constitutively in many tissues and is thought to mediate most of the biological actions of BK.^{2,4}

BK exhibits highly potent and diverse proinflammatory activities and is believed to play important roles in a variety of inflammatory diseases including asthma, rhinitis, pancreatitis, sepsis, rheumatoid arthritis, brain edema, angioneurotic edema, hepatorenal syndrome,⁸ and ulcerative colitis.⁹ Recently, it was also suggested that BK may be involved in the pathology of small-cell lung cancer (SCLC),^{10,11} bacterial and viral infections,^{12,13} and Alzheimer's disease.¹⁴ Therefore, the development of specific BK antagonists has been of great importance for investigating the pathophysiological roles of BK and for developing a novel class of therapeutic drugs.

Since the discovery of the first peptide BK B₂ receptor antagonist, NPC567 ([D-Arg⁰, Hyp³, D-Phe⁷]BK), by Vavrek and Stewart in 1985,¹⁵ a number of peptide B₂

* To whom correspondence should be addressed. Phone: +81-6-6390-1247. Fax: +81-6-6304-5385. E-mail: hiroshi_kayakiri@po.fujisawa.co.jp.

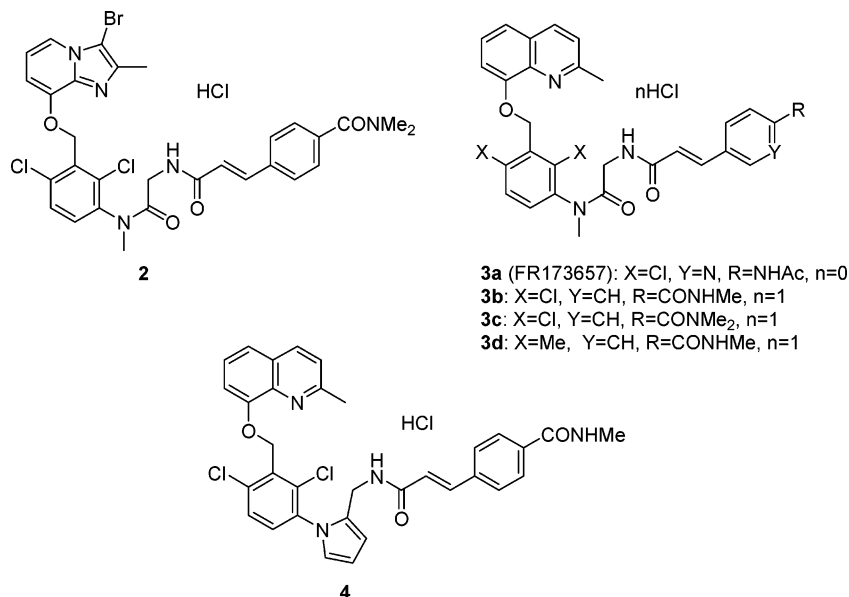
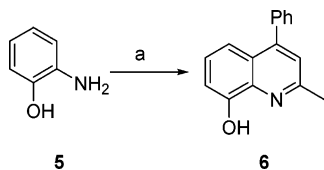
[†] Present address: Medicinal Chemistry Research Laboratories, Fujisawa Pharmaceutical Co. Ltd., 5-2-3 Tokodai, Tsukuba, Ibaraki 300-2698, Japan.

[‡] Present address: Research Division, Fujisawa Pharmaceutical Co. Ltd., 2-1-6, Kashima, Yodogawa-ku, Osaka 532-8514, Japan.

[§] Present address: Medicinal Chemistry Research Laboratories, Fujisawa Pharmaceutical Co. Ltd., 2-1-6, Kashima, Yodogawa-ku, Osaka 532-8514, Japan.

[#] Present address: Medicinal Biology Research Laboratories, Fujisawa Pharmaceutical Co. Ltd., 2-1-6, Kashima, Yodogawa-ku, Osaka 532-8514, Japan.

[†] Present address: Faculty of Pharmaceutical Sciences, Setsunan University, 45-1, Nagaotoge-cho, Hirakata, Osaka 573-0101, Japan.

Chart 2. Representative Fujisawa Non-Peptide B₂ Antagonists (**2**, **3a–d**, and **4**)**Scheme 1^a**

^a Reagents: (a) 1-phenyl-2-buten-1-one, concentrated HCl.

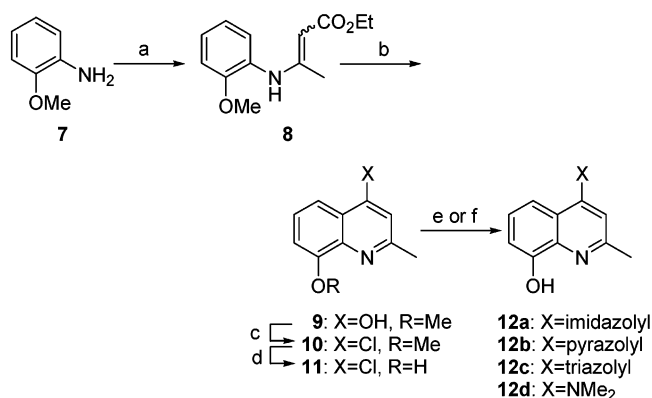
antagonists have been synthesized,^{16–20} including the clinically evaluated second-generation antagonists **1** (HOE140; icatibant; [D-Arg⁰, Hyp³, Thi⁵, D-Tic⁷, Oic⁸]BK) and CP0127 (bradycor) (Chart 1). On the other hand, WIN64338 was disclosed as the first non-peptide B₂ antagonist in 1993.²¹ However, this compound was not so selective²² and was practically inactive against the B₂ receptor in isolated human umbilical vein.²³ In 1996, we presented **3a** (FR 173657) as the first potent, selective, and orally active non-peptide BK B₂ receptor antagonist. Since then, we have reported several novel classes of non-peptide B₂ antagonists,^{24–30} represented by **2**, **3b,c**, and **4** (Chart 2). Recently, several new pseudopeptide^{31–33} and non-peptide^{34–39} compounds were described as B₂ receptor antagonists.

We recently initiated a new research program to discover non-peptide B₂ antagonists that would be suitable for intravenous infusion for the treatment of life-threatening inflammatory disorders such as acute pancreatitis, septic shock, and traumatic brain edema. Herein, we report the SAR and new insights into species difference revealed in the course of discovery of a new class of highly potent non-peptide B₂ antagonists with improved aqueous solubility.

Chemistry

The compounds described herein are presented in Tables 1–3, and the methods for their syntheses are outlined in Schemes 1–7.

Schemes 1 and 2 show the synthetic routes for the 4-substituted quinolinol derivatives. Cyclization of 2-aminophenol (**5**) with 1-phenyl-2-buten-1-one provided 2-methyl-4-phenyl-8-quinolinol (**6**) (Scheme 1).

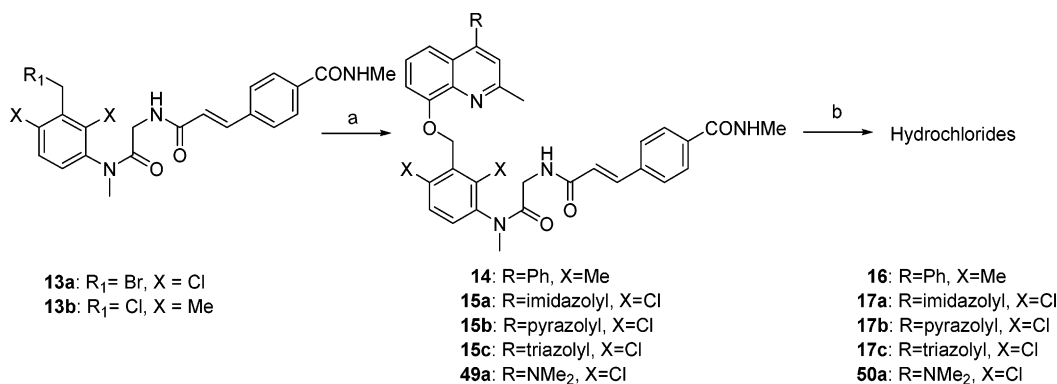
Scheme 2^a

^a Reagents: (a) ethyl acetoacetate, AcOH, benzene; (b) biphenyl, phenyl ether, 235 °C; (c) PhNMe₂, POCl₃, reflux; (d) BBr₃, CH₂Cl₂; (e) five-membered heterocycles, 1,4-dioxane, reflux; (f) DMF, reflux.

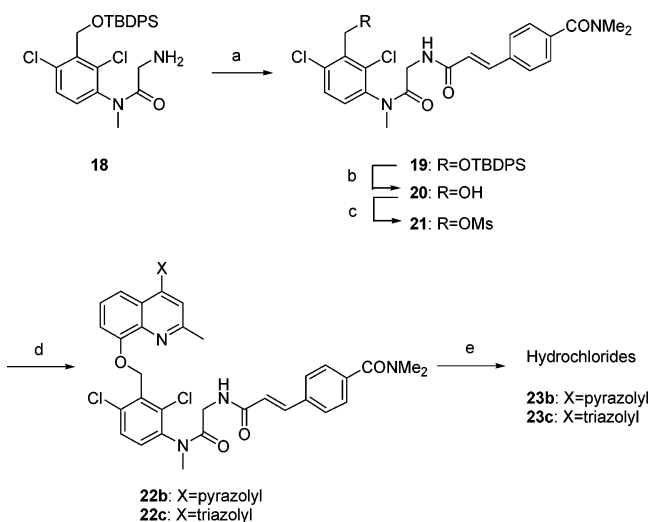
The crotonate **8**, which was prepared by condensing *o*-anisidine (**7**) with ethyl acetoacetate, was cyclized to give **9**. The quinolinol **9** was treated with phosphorus oxychloride to give the 4-chloroquinoline **10**, which was deprotected to yield **11**. The quinolinol **11** was heated with imidazole, pyrazole, or triazole in 1,4-dioxane to give **12a**, **12b**, or **12c**, respectively. On the other hand, 4-(dimethylamino)-2-methyl-8-quinolinol (**12d**) was obtained from **11** by heating in DMF (Scheme 2).

The quinolinols **6** and **12a–d** were coupled with the benzyl bromide **13a**²⁶ or the benzyl chloride **13b**²⁶ in the presence of K₂CO₃ to give **14**, **15a–c**, and **49a**, respectively. The 4-substituted quinoline derivatives **14**, **15a–c**, and **49a** were treated with 10% HCl in MeOH to afford the corresponding hydrochlorides **16**, **17a–c**, and **50a**, respectively (Scheme 3).

Preparation of the 4-pyrazol-1-yl or the 4-triazol-1-yl derivatives **23b** and **23c** are shown in Scheme 4. The amine **18**²⁶ was acylated and deprotected to provide the benzyl alcohol **20**. Treatment of **20** with methanesulfonyl chloride and successive condensation with the quinolinols **12b** and **12c** yielded the 4-heteroaromatic quinoline derivatives **22b** and **22c**, respectively. The compounds **22b** and **22c** were treated with 10% HCl in

Scheme 3^a

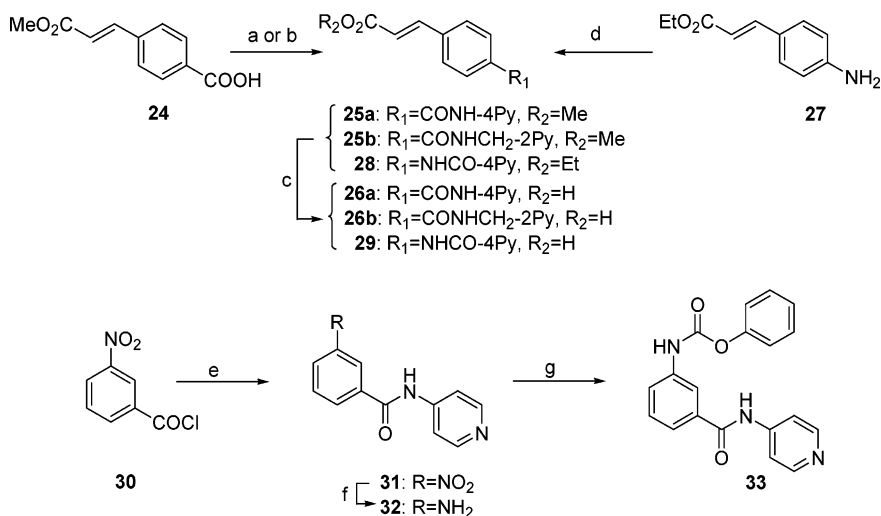
^a Reagents: (a) 4-substituted quinolinols (**6**, **12a–d**), K₂CO₃, DMF; (b) 10% HCl/MeOH.

Scheme 4^a

^a Reagents: (a) (*E*)-4-(*N,N*-dimethylcarbamoyl)cinnamic acid, WSCD·HCl, HOBT, DMF; (b) *n*-Bu₄NF, THF; (c) MsCl, Et₃N, CH₂Cl₂; (d) 4-substituted quinolinols (**12b** or **12c**), K₂CO₃, DMF; (e) 10% HCl/MeOH.

MeOH to afford the corresponding hydrochlorides **23b** and **23c**, respectively.

The fragments of the terminal cinnamide and ureas were prepared as shown in Scheme 5. The cinnamate

Scheme 5^a

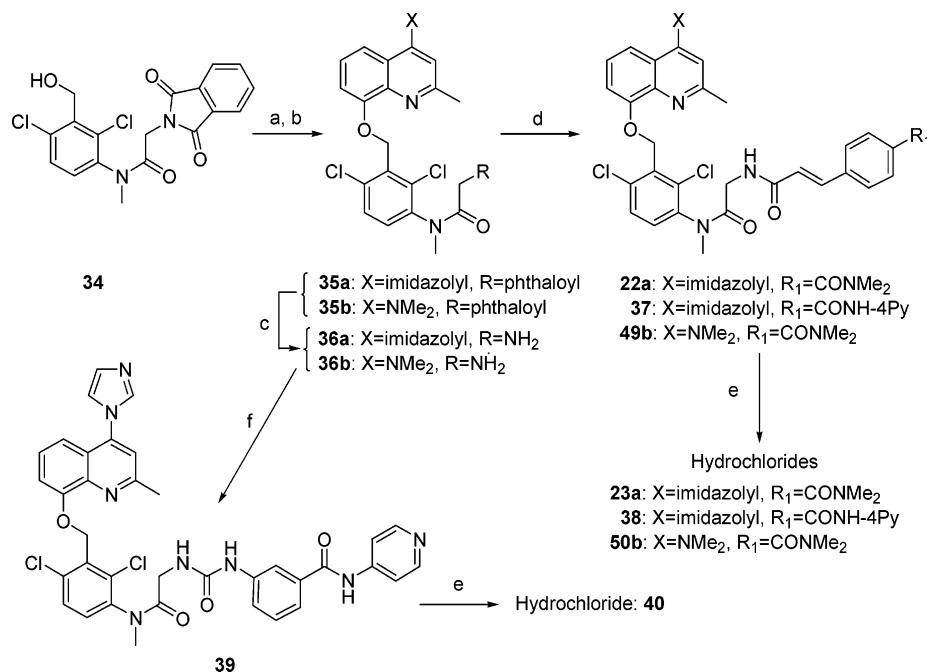
^a Reagents: (a) SOCl₂, DMF, RNH₂; (b) RNH₂, WSCD·HCl, HOBT, DMF; (c) 1 N NaOH, MeOH; (d) isonicotinoyl chloride, Et₃N, CH₂Cl₂; (e) 4-aminopyridine, Et₃N, CH₂Cl₂; (f) H₂, Pd/C, MeOH, 1,4-dioxane; (g) phenyl chloroformate, 1 N NaOH, 1,4-dioxane.

25a was obtained from the acid **24**²⁵ via its acid chloride. On the other hand, condensation of **24** with 2-(amino-methyl)pyridine gave methyl (*E*)-4-[(2-pyridinylmethyl)-amino]carbonylcinnamate (**25b**). The methyl esters **25a** and **25b** were hydrolyzed to give (*E*)-4-(substituted)-cinnamic acids **26a** and **26b**, respectively. Ethyl (*E*)-4-aminocinnamate (**27**)²⁵ was treated with isonicotinoyl chloride and was saponified to give the acid **29**. Coupling of 3-nitrobenzoyl chloride (**30**) with 4-aminopyridine followed by reduction of the nitro group and treatment with phenyl chloroformate yielded the phenyl carbamate **33**.

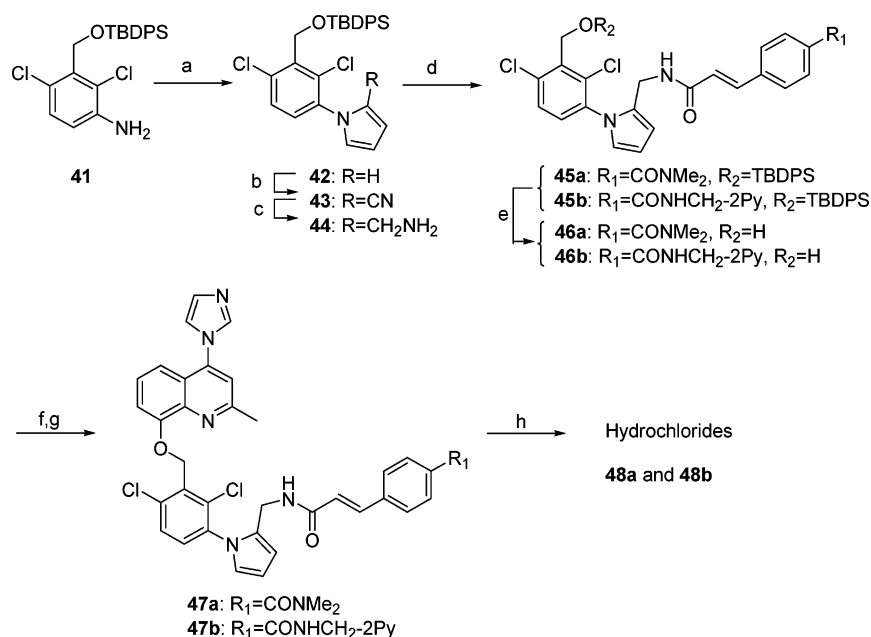
Modifications of the terminal cinnamide moiety of the 4-(imidazol-1-yl) or 4-dimethylaminoquinoline derivatives are shown in Scheme 6. The benzyl alcohol **34** was mesylated and coupled with the quinolinols **12a** and **12d** to give **35a** and **35b**, respectively. Removal of the *N*-phthaloyl groups of **35a** and **35b** and coupling with (*E*)-4-(substituted)cinnamic acids afforded the corresponding cinnamides **22a**, **37**, and **49b**. They were treated with 10% HCl in MeOH to afford the corresponding hydrochlorides **23a**, **38**, and **50b**.

On one hand, the amine **36a** was coupled with phenylcarbamate **33** and was treated with 10% HCl in MeOH to give the hydrochloride **40** (Scheme 6).

Preparation of 4-(substituted)pyrrole derivatives **48a** and **48b** is outlined in Scheme 7. The pyrrole **42** was

Scheme 6^a

^a Reagents: (a) MsCl, Et₃N, CH₂Cl₂; (b) **12a** or **12d**, *n*-Bu₄NI, K₂CO₃, DMF; (c) N₂H₄·H₂O, EtOH; (d) 4-substituted cinnamic acid, WSCD·HCl, HOBT, DMF; (e) 10% HCl/MeOH; (f) **33**, Et₃N, DMF, 80 °C.

Scheme 7^a

^a Reagents: (a) 2,5-dimethoxytetrahydrofuran, AcOH, 90 °C; (b) ClSO₂NCO, DMF, CH₂Cl₂; (c) LAH, THF; (d) 4-substituted cinnamic acid, WSCD·HCl, HOBT, DMF; (e) *n*-Bu₄NF, THF; (f) MsCl, Et₃N, CH₂Cl₂; (g) **12a**, K₂CO₃, DMF; (h) 10% HCl/MeOH.

obtained from the aniline **41**²⁶ by heating with 2,5-dimethoxytetrahydrofuran in AcOH. Reaction of **42** with chlorosulfonyl isocyanate provided the 2-cyano derivative **43**. The cyano group of **43** was reduced to give the amine **44**, which was condensed with the (*E*)-4-(substituted)cinnamic acids followed by deprotection to give the benzyl alcohols **46a** and **46b**, respectively. Reaction of the benzyl alcohols **46a** and **46b** with methanesulfonyl chloride and successive condensation with **12a** yielded the quinoline derivatives **47a** and **47b**, which were converted to the corresponding hydrochlorides **48a** and **48b**, respectively.

Computational Chemistry

Molecular Modeling. All computational studies were performed using the molecular modeling program SYBYL 6.7,⁴⁰ running on a Silicon Graphics Octane workstation. Structures were energy-minimized using a conjugate gradient minimization algorithm with the Tripos force field⁴¹ until a gradient convergence of 0.001 kcal/(mol·Å) was reached, without solvent, using default parameters. Partial atomic charges of the molecules were calculated using the PM3 model Hamiltonian within MOPAC 6.0.⁴²

Compound Selection and Alignment. Twenty-four compounds, incorporating various heteroaromatic groups as the "quinoline part" and the common benzyl moiety of **3b**, were selected from our non-peptide B₂ antagonist library.^{25,26} Their structures and binding affinities for human and guinea pig B₂ receptors are summarized in Table 2. The alignment was performed using the heavy atoms of the identical substituent by least-squares fitting.

Biology

All compounds were tested for inhibition of the specific binding of [³H]BK to the B₂ receptor in guinea pig ileum membrane preparations as previously reported,^{24,25,28–30} and they were also evaluated for inhibition of the specific binding of [³H]BK to the cloned human B₂ receptor expressed in Chinese hamster ovary (CHO) cells.²⁹ Selected compounds were then tested for in vivo functional antagonistic activity in inhibiting BK-induced bronchoconstriction in guinea pigs by intravenous administration.^{24,25,28,30} Pharmacokinetics by intravenous administration of the representative compound was also studied in rats.

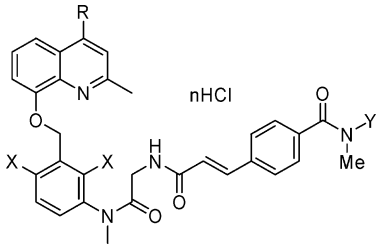
Results and Discussion

We reported earlier the first selective and orally active non-peptide BK B₂ receptor antagonists with subnanomolar affinities for both human and guinea pig B₂ receptors, incorporating 8-[[2,6-dichloro-3-[*N*-substituted]benzyl]oxy]-2-methylimidazo[1,2-*a*]pyridine and 8-[[2,6-dichloro-3-[*N*-substituted]benzyl]oxy]-2-methylquinoline frameworks.^{24–27,43} Representative compounds significantly inhibited BK-induced bronchoconstriction in guinea pigs by oral administration at 0.1 mg/kg or less; however, it was difficult to administer them intravenously because of poor aqueous solubility. The saturated concentration of **3b** was 0.55 mg/mL even in a pH 2 buffer. Therefore, we started a new research program to improve the aqueous solubility of our non-peptide B₂ antagonists, aiming at development of novel therapeutic drugs that could be administered by intravenous infusion for the treatment of life-threatening inflammatory disorders such as acute pancreatitis, septic shock, and traumatic brain edema.

The amino acid sequence of the B₂ receptors is highly conserved between species. For example, the guinea pig B₂ receptor is reported to share high sequence homology with the human (81.5%), rat (82.6%), mouse (81.5%), and rabbit (80.7%) B₂ receptors.⁴⁴ However, the pharmacological profiles of the B₂ receptors to various ligands are markedly different.⁴⁵ Therefore, it is essential to overcome this "binding paradox"⁴⁵ in order to develop a B₂ ligand as a therapeutic drug. As part of our efforts to address this issue, we have carefully investigated the SAR for both human and guinea pig B₂ receptors.

Since a halogen atom at the 3-position of the imidazo[1,2-*a*]pyridine ring in our former series enhanced binding affinities for the human and guinea pig B₂ receptors, we presumed that both B₂ receptors could accommodate a rather large substituent around the 4-position of the quinoline ring. As a probe, the 4-phenyl derivative **16** was synthesized and inhibition of the specific binding of [³H]BK to cloned human and guinea

Table 1. Introduction of 4-Substituents



compds	R	X	Y	n	in vitro IC ₅₀ (nM)	
					guinea pig ileum ^a	cloned human B ₂ ^b
3b	H	Cl	H	0	0.51 ^c	1.1 ^c
3d	H	Me	H	1	0.97 ^c	4.8 ^c
16	Ph	Me	H	1	3.1	1.0
17a	1-imidazolyl	Cl	H	2	3.7	0.28
17b	1-pyrazolyl	Cl	H	2	2.7	0.17
17c	1-triazolyl	Cl	H	2	4.4	0.23
3c	H	Cl	Me	1	1.3 ^c	3.9 ^c
23a	1-imidazolyl	Cl	Me	2	4.3	0.35
23b	1-pyrazolyl	Cl	Me	2	3.3	0.18
23c	1-triazolyl	Cl	Me	2	9.1	0.28
50a	NMe ₂	Cl	H	2	1.8	3.2
50b	NMe ₂	Cl	Me	2	2.9	2.1

^a Concentration required to inhibit specific binding of [³H]BK (0.06 nM) to the B₂ receptor in guinea pig ileum membrane preparations by 50%. Values are expressed as the average of at least three determinations, with variation in individual values of <15%. See the Experimental Section for further details. ^b Concentration required to inhibit specific binding of [³H]BK (1.0 nM) to the human B₂ receptor that was expressed in CHO cells by 50%. Values are expressed as the average of at least three determinations, with variation in individual values of <15%. See the Experimental Section for further details. ^c Previously published (see ref 26).

pig B₂ receptors was evaluated (Table 1). As a result, **16** displayed nanomolar affinity for both human and guinea pig B₂ receptors, indicating that both B₂ receptors have sufficient space to accommodate 4-substituents on the quinoline ring. Specifically, its IC₅₀ values for the human and guinea pig B₂ receptors are 5 times lower and 3 times higher, respectively, compared with those of the 4-H counterpart **3d**. The 4-phenyl group seems to be favorable for binding to the human B₂ receptor and unfavorable for binding to the guinea pig B₂ receptor.

As the next step, we investigated conversion of the phenyl group of **16** to heteroaromatic rings containing nitrogen atoms, aiming to improve aqueous solubility. Introduction of 1-imidazolyl, 1-pyrazolyl, and 1-triazolyl moieties to the 4-position of the quinoline ring of compounds **3b** and **3c** afforded highly potent ligands **17a–c** and **23a–c**, respectively. These compounds displayed excellent subnanomolar binding affinities for the human B₂ receptor compared with the low nanomolar affinities of parent compounds **3b** and **3c**. In contrast, affinities for the guinea pig B₂ receptor were several times lower than those of **3b** and **3c**. The quite similar in vitro profiles of imidazole, pyrazole, and triazole derivatives suggested that the 2-, 3-, and 4-nitrogen atoms on the heterocyclic rings do not make important contributions to binding. To elucidate the effect of the common 1-nitrogen atom, 4-dimethylamino derivatives **50a** and **50b** were investigated. They showed low nanomolar binding affinities for both human and guinea pig B₂ receptors, indicating that the nitrogen

Table 2. Test Set of Benzamide Derivatives Used To Test the Predictive Ability of the CoMFA Model

R
O
X
X
nHCl
CONHMe

comps	R	X	n	IC ₅₀ (nM)		comps	R	X	n	IC ₅₀ (nM)	
				GP ileum ^a	Cloned Human B ₂ ^b					GP ileum ^a	Cloned Human B ₂ ^b
51a		Cl	1	0.50 ^c	9.0 ^c	51m		Me	0	9.5 ^d	79 ^d
51b		Cl	0	380 ^d	1100 ^d	51n		Me	0	94 ^d	670 ^d
51c		Cl	0	9.1 ^d	67 ^d	51o		Me	0	38 ^d	160 ^d
51d		Cl	0	23 ^d	270 ^d	51p		Cl	0	110 ^d	56 ^d
51e		Cl	0	8.9 ^d	48 ^d	51q		Cl	1	1.0 ^d	5.2 ^d
51f		Cl	1	8.7 ^d	22 ^d	51r		Cl	0	170 ^d	2900 ^d
51g		Cl	0	0.83 ^d	2.2 ^d	3b		Cl	1	0.51	1.1
51h		Me	0	1.6 ^d	7.2 ^d	3d		Me	1	0.97	4.8
51i		Me	0	90 ^d	730 ^d	16		Me	1	3.1	1.0
51j		Me	0	1000 ^d	9100 ^d	17a		Cl	2	3.7	0.28
51k		Me	0	1100 ^d	8400 ^d	17b		Cl	2	2.7	0.17
51l		Me	0	200 ^d	94 ^d	17c		Cl	2	4.4	0.23

^a Concentration required to inhibit specific binding of [³H]BK (0.06 nM) to the B₂ receptor in guinea pig ileum membrane preparations by 50%. Values are expressed as the average of at least three determinations, with variation in individual values of <15%. See the Experimental Section for further details. ^b Concentration required to inhibit specific binding of [³H]BK (1.0 nM) to the human B₂ receptor that was expressed in CHO cells by 50%. Values are expressed as the average of at least three determinations, with variation in individual values of <15%. See the Experimental Section for further details. ^c Previously published (see ref 25). ^d Previously published (see ref 26).

atom at the 4-position of the quinoline ring does not contribute to the species difference. On the basis of these results, we speculated that the imidazolyl, pyrazolyl, and triazolyl moieties could increase binding affinity for the human B₂ receptor and decrease that for the guinea pig B₂ receptor mainly in a steric manner.

To obtain more detailed information on SAR around the quinoline moiety, we carried out a CoMFA⁴⁶ study

using SYBYL, version 6.7, using 24 compounds chosen from our B₂ ligand library on the basis of the structural features in the "quinoline part". Table 2 summarizes their structures and binding affinities. In the analysis of binding affinities for the human B₂ receptor, the CoMFA-derived QSAR models exhibited considerably correlative and predictive properties. A cross-validated $r^2 = 0.643$ with five components and a non-cross-

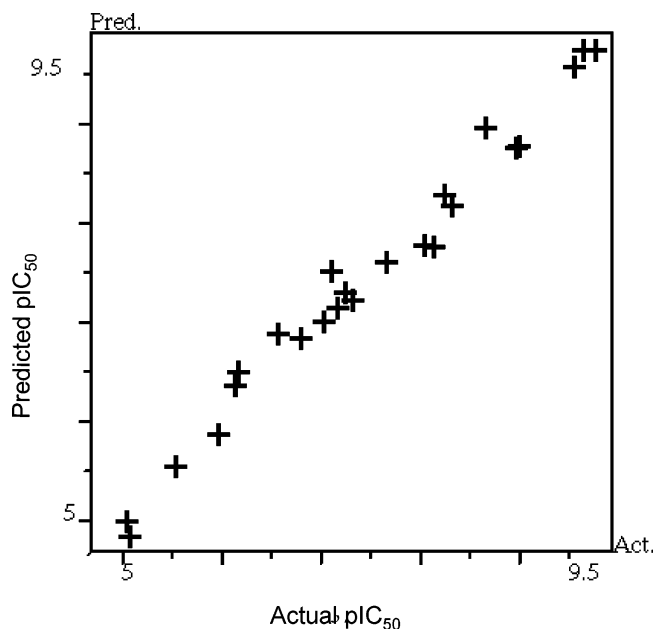


Figure 1. CoMFA predicted vs experimental pIC₅₀ values.

validated $r^2 = 0.979$ with $F = 167.20$ ($n_1 = 5$, $N_2 = 18$) were observed with the model. The graph depicting the calculated vs observed activities of the molecules used in building the QSAR model is shown in Figure 1. In this analysis, steric fields were observed to be more contributive than electrostatic fields (steric:electrostatic = 0.62:0.38). A bootstrap analysis (100 samples) was performed to obtain the confidence limits for this analysis. An r^2 bootstrap of 0.986 with a standard deviation of 0.007 suggested that a similar relationship exists for all compounds.

The model with 2 Å grid spacing was further validated to assess its predictive power. The effect of the alignment relative to the grid position was investigated by consistently moving all compounds in increments of 0.5

Å. The $r^2(cv)$ values for each orientation ranged from 0.52 to 0.62, suggesting a slight dependence of the model on absolute orientation. The effect of the grid size was tested by the calculation at 2 Å (default) and 1 Å grid distances. No significant differences were found between the models obtained at 2 or 1 Å grid distances (for 2 Å, $r^2(cv) = 0.643$; for 1 Å, $r^2(cv) = 0.608$).

Figure 2 illustrates steric and electrostatic fields generated by CoMFA. The steric and electrostatic fields were analyzed for areas that might improve binding affinity with changes in substituent sizes or charges. The green (sterically favorable) and yellow (sterically unfavorable) contours represent 80% and 20% level contributions, respectively. Figure 2 also shows CoMFA electrostatic fields, with blue and red regions indicative of areas where affinity could be improved by more positively and negatively charged substituents, respectively. The blue and red contours represent 80% and 20% level contributions, respectively. Examination of the CoMFA steric and electrostatic map revealed that near the 4-substituent of the quinoline ring, a favorable steric region was located and no electrostatic region was found, supporting the speculation discussed above. On the other hand, in the CoMFA study of binding affinities for the guinea pig B₂ receptor, no correlative or predictive CoMFA-derived QSAR model was obtained. Trials to modify the methods of charge calculations, grid spacing, CoMFA regions, and filtering in the PLS calculation were performed, but the best cross-validated r^2 was 0.19. This result shows that affinities for the guinea pig B₂ receptor could not be explained by only steric and electrostatic interactions, clearly indicating the species difference between the human and guinea pig B₂ receptors.

A preliminary solubility study of these 4-substituted derivatives was carried out to assess the possibility for intravenous administration. Among the tested 4-aryl-substituted derivatives, only the imidazole derivative

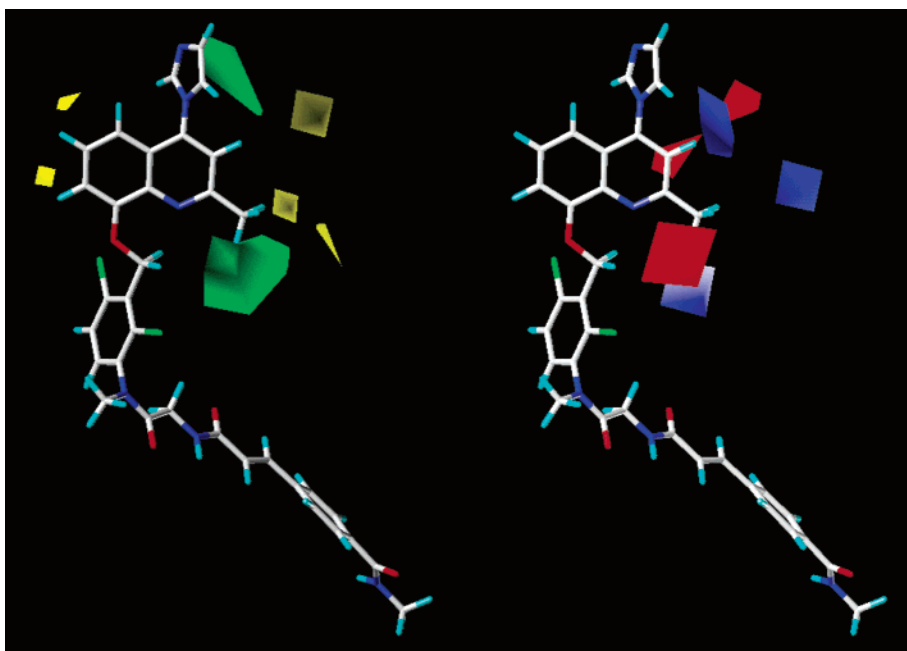
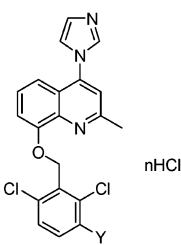
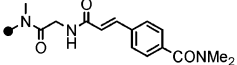
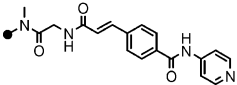
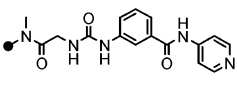
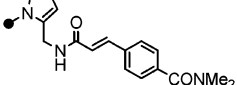
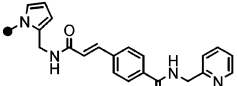


Figure 2. Contour map of steric and electrostatic fields from the B₂ receptor CoMFA models. Color coding is as follows: blue = positive charge favors high affinity; red = negative charge favors high affinity; green = steric bulk favors high affinity; yellow = steric bulk does not favor high affinity.

Table 3. Representative Imidazolyl Derivatives with Improved Aqueous Solubility


comps	Y	n	IC ₅₀ (nM)		Inhibition (%) against BK-induced bronchoconstriction (iv) ^c	
			GP ileum ^a	Cloned Human B ₂ ^b	1 μg/kg	10 μg/kg
23a		2	4.3	0.35	NT ^d	56.5±13.5*
38		3	17	0.42	NT	42.5±2.5*
40		3	6.6	0.23	NT	56.8±3.9*
48a		2	3.0	0.26	46.0±7.8**	78.6±7.7**
48b		3	6.0	0.43	NT	50.0±7.9*
1			0.090	0.49	63.4±8.9**	96.7±0.3***

^a Concentration required to inhibit specific binding of [³H]BK (0.06 nM) to the B₂ receptor in guinea pig ileum membrane preparations by 50%. Values are expressed as the average of at least three determinations, with variation in individual values of <15%. See the Experimental Section for further details. ^b Concentration required to inhibit specific binding of [³H]BK (1.0 nM) to the human B₂ receptor that was expressed in CHO cells by 50%. Values are expressed as the average of at least three determinations, with variation in individual values of <15%. See the Experimental Section for further details. ^c BK (5 μg/kg) was administered intravenously to anesthetized guinea pigs, and bronchoconstriction induced by the BK administration was measured by the modified Konzett and Rössler method⁴⁸ as previously reported. After 5 min, compounds were intravenously administered. After 25 min, BK was administered again and bronchoconstriction was measured. Percent inhibition was calculated from the values of percent responses of drug-treated and controlled groups (*n* = 3–4). The results are expressed as the mean ± SEM: (*) *P* < 0.05, (**) *P* < 0.01, (***) *P* < 0.001 vs control (Student's *t*-test). See the Experimental Section for further details. ^d NT, not tested.

23a could be dissolved up to 10 mg/mL in a 5% aqueous solution of citric acid. Thus, we investigated further optimization of the 4-imidazolyl series. As shown in Table 3, introduction of representative side chains, identified in our previous studies, to the 3-position of the benzyl moiety afforded highly potent ligands **38**, **40**, **48a**, and **48b** for the human B₂ receptor with subnanomolar IC₅₀ values. On the other hand, their binding affinities for the guinea pig B₂ receptor were 3–17 times lower than that of the 4-H derivative **3b**, indicating the species difference more clearly. All of them could be dissolved in a 5% aqueous solution of citric acid at up to 10 mg/mL, indicating potential for iv administration.

Compounds **23a**, **38**, **40**, **48a**, and **48b** did not affect by themselves the formation of the second messenger inositol phosphates in CHO cells expressing the cloned human B₂ receptor up to 10 μM, indicating that they do not have agonistic or inverse agonistic properties (data not shown). Furthermore, their antagonistic properties were proven in vivo. We used a BK-induced bronchoconstriction model in guinea pigs for quick and precise in vivo screening. Compounds **23a**, **38**, **40**, **48a**,

and **48b** significantly inhibited BK-induced bronchoconstriction in guinea pigs by intravenous administration at 10 μg/kg or less. In particular, the pyrrole derivative **48a** exhibited comparable inhibitory activity to that of **1**, a representative second-generation peptide B₂ antagonist, even at 1 μg/kg (iv), despite its more than 30 times lower binding affinity for the guinea pig B₂ receptor compared with that of **1**. Since its binding affinity for the human B₂ receptor is superior to that of **1**, we expect that compound **48a** should be more effective than **1** in the clinic. In a preliminary pharmacokinetic study in rats, **48a** showed a *t*_{1/2} value of 22 min at 3.2 mg/kg (iv) (Figure 3).

Further investigations of the 4-substituent of the quinoline ring are revealing its critical role in determining agonist/antagonist profiles. These studies will be reported in due course.

Conclusions

The 4-phenylquinoline derivative **16** revealed that human and guinea pig B₂ receptors have a pocket that can accommodate rather large substituents at the

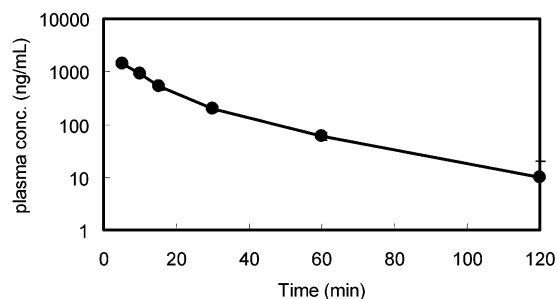


Figure 3. 48a plasma concentration–time curve.

4-position of the quinoline ring. Introduction of various heteroaromatic substituents at this position enabled discovery of a new class of highly potent non-peptide B₂ receptor antagonists. For the human B₂ receptor, the 4-heteroaromatic substituents functioned as a new pharmacophore and increased binding affinities, although they reduced those for the guinea pig receptor, indicating the species difference between human and guinea pig B₂ receptors. CoMFA studies suggested that the 4-heteroaromatic substituents increased binding affinities for the human B₂ receptor mainly in a steric manner and that there is a clear species difference between the human and guinea pig B₂ receptors. The 4-(1-imidazolyl) derivatives **23a**, **38**, **40**, **48a**, and **48b** could be dissolved in a 5% citric acid aqueous solution up to 10 mg/mL and significantly inhibited BK-induced bronchoconstriction in guinea pigs by intravenous administration at 10 μg/kg. In particular, **48a** afforded comparable potency in vivo to that of **1**, despite its more than 30 times lower binding affinity for the guinea pig B₂ receptor compared to that of **1**. Since **48a** exhibited superior affinity for the human B₂ receptor compared to **1**, it is expected that this compound should be more potent than **1** in the clinic.

Experimental Section

Chemistry. Melting points were determined on a Mel-Temp instrument (Mitamura Riken Kogyo, Japan) and are uncorrected. Proton NMR spectra were recorded at 200 or 300 MHz with a Bruker AM200 or a Varian Gemini 300 spectrometer, and chemical shifts are expressed in δ (ppm) with TMS as the internal standard. The peak patterns are shown as the following abbreviations: s = singlet, d = doublet, t = triplet, q = quartet, m = multiplet, br = broad. The mass spectra (MS) were recorded with a VG (Fisons) ZAB-SE (FAB) or Micromass Platform (ESI) system. Elemental analyses were performed on a Perkin-Elmer 2400 CHN analyzer. Analytical results were within ±0.4% of the theoretical values unless otherwise noted. Silica gel thin-layer chromatography was performed on pre-coated plates Kieselgel 60F₂₅₄ (E. Merck, AG, Darmstadt, Germany). Silica gel flash chromatography was performed with Kieselgel 60 (230–400 mesh) (E. Merck, AG, Darmstadt, Germany). Yields were not optimized.

Computational Chemistry. CoMFA Interaction Energies. The CoMFA grid spacing was 2.0 Å in the *x*, *y*, and *z* directions, and the grid region was automatically generated by the CoMFA routine to encompass all molecules with an extension of 4.0 Å in each direction. An sp³ carbon and a charge of +1.0 were used as probes to generate the interaction energies at each lattice point. The steric and electrostatic contributions were truncated to ±30 kcal/mol, and the electrostatic contributions were ignored at lattice intersections with maximal steric interactions.

Partial Least Squares Analysis. The partial least-squares algorithm was used in conjugation with the cross-validation (leave one out) option to obtain the optimum number of

components, which were used to generate the final CoMFA model without cross-validation. Equal weights were assigned to steric and electrostatic descriptors using the CoMFA scaling option. All cross-validated PLS analyses were performed with a minimum value of 2.0 kcal/mol, which minimized the influence of column noise and reduced the computation time. To obtain the statistical confidence limits on the analysis, PLS analysis using 100 bootstrap groups was performed with randomly interchanged biological activity.

2-Methyl-4-phenyl-8-quinolinol (6). To a suspension of 2-aminophenol (**5**) (2.00 g, 18.3 mmol) in concentrated HCl (8 mL) was added dropwise 1-phenyl-2-buten-1-one (8.03 g, 55.0 mmol) at 100 °C. This mixture was refluxed for 24 h, cooled to 0 °C, adjusted to pH 7 with 28% ammonium hydroxide solution, and extracted with CHCl₃. The organic layer was washed with brine, dried over MgSO₄, and evaporated in vacuo. The residue was purified by flash silica gel chromatography (CHCl₃/MeOH, 97:3) to afford **6** (2.40 g, 55.7%) as a brown oil: ¹H NMR (300 MHz, CDCl₃) δ 2.75 (s, 3H), 7.14 (m, 1H), 7.27–7.36 (m, 2H), 7.40–7.61 (m, 6H), 7.95 (d, *J* = 8 Hz, 1H); MS (ESI) *m/z* 236 (M + 1). Anal. (C₁₆H₁₃NO) C, H, N.

Ethyl (2*E*)-3-(2-Methoxyanilino)-2-butenolate or Ethyl (2*Z*)-3-(2-Methoxyanilino)-2-butenolate (8). A solution of *o*-anisidine (**7**) (30.0 g, 0.244 mol), ethyl acetoacetate (31.7 g, 0.244 mol), and AcOH (1 mL) in benzene (90 mL) was refluxed for 8 h, removing water with a Dean–Stark apparatus. This mixture was cooled to room temperature and concentrated in vacuo. The residue was purified by flash silica gel chromatography (hexane/EtOAc, 20:1) to afford **8** (57.2 g, 99.8%) as a pale-yellow oil: ¹H NMR (300 MHz, CDCl₃) δ 1.29 (t, *J* = 7.5 Hz, 3H), 2.00 (s, 3H), 3.86 (s, 3H), 4.15 (q, *J* = 7.5 Hz, 2H), 4.71 (s, 1H), 6.82–6.93 (m, 2H), 7.02–7.16 (m, 2H). Anal. (C₁₃H₁₇NO₃) C, H, N.

8-Methoxy-2-methyl-4-quinolinol (9). To a mixture of biphenyl (90 g) and phenyl ether (90 mL) was added dropwise **8** (60.2 g, 0.256 mol) at 230–235 °C over 15 min. After 3 h of being stirred at 235 °C, the reaction mixture was cooled at room temperature. The mixture was diluted with hexane (200 mL) and the precipitate was collected by vacuum filtration followed by crystallization from CH₃CN to afford **9** (23.6 g, 48.7%) as pale-brown crystals: mp 230–232 °C; ¹H NMR (300 MHz, DMSO-*d*₆) δ 2.38 (s, 3H), 3.99 (s, 3H), 5.90 (s, 1H), 7.18–7.23 (m, 2H), 7.54–7.63 (m, 1H). Anal. (C₁₁H₁₁NO₂) C, H, N.

4-Chloro-8-methoxy-2-methylquinoline (10). To a suspension of 8-methoxy-2-methyl-4-quinolinol (**9**) (23.5 g, 0.124 mol) in phosphorus oxychloride (92 mL, 0.987 mol) was added dropwise *N,N*-dimethylaniline (31.5 mL, 0.248 mol) in an ice/water bath over 20 min under nitrogen. After 15 min, the reaction mixture was stirred at ambient temperature for 2 h and refluxed for 2 h. The reaction mixture was concentrated in vacuo, adjusted to pH 8 with saturated aqueous NaHCO₃ and extracted with CH₂Cl₂ twice. The organic layer was washed with saturated aqueous NaHCO₃, water, and brine, dried over MgSO₄, and evaporated in vacuo. The residue was purified by flash silica gel column chromatography (CH₂Cl₂/EtOAc, 5:1) followed by crystallization from hexane to afford **10** (21.1 g, 81.9%) as pale-yellow crystals: mp 80–82 °C; ¹H NMR (300 MHz, CDCl₃) δ 2.78 (s, 3H), 4.09 (s, 3H), 7.10 (d, *J* = 8 Hz, 1H), 7.44 (s, 1H), 7.50 (dd, *J* = 8, 8 Hz, 1H), 7.75 (d, *J* = 8 Hz, 1H). Anal. (C₁₁H₁₀ClNO) C, H, N.

4-Chloro-2-methyl-8-quinolinol (11). To a solution of 4-chloro-8-methoxy-2-methylquinoline (**10**) (16.0 g, 77 mmol) in dry CH₂Cl₂ (160 mL) was added dropwise boron tribromide (38.6 g, 154 mmol) below –50 °C under nitrogen. After 15 min, the reaction mixture was stirred at ambient temperature for 2 h and refluxed for 2 h. The cooled mixture was adjusted to pH 8 with saturated aqueous NaHCO₃ and stirred in an ice/water bath for 4 h. The organic layer was separated, and the water layer was extracted with CH₂Cl₂. The organic layer was combined, washed with water and brine, dried over MgSO₄, and evaporated in vacuo. The residue was dissolved in CH₂Cl₂ (100 mL), and silica gel (5 g) was added to the solution. The mixture was stirred at ambient temperature for 1 h, and silica gel was removed by filtration. The filtrate was concentrated

in vacuo followed by crystallization from hexane to afford **11** (10.5 g, 70.4%) as pale-yellow crystals: mp 57–59 °C; ¹H NMR (300 MHz, CDCl₃) δ 2.70 (s, 3H), 7.20 (d, *J* = 8 Hz, 1H), 7.40 (s, 1H), 7.47 (dd, *J* = 8, 8 Hz, 1H), 7.61 (d, *J* = 8 Hz, 1H). Anal. (C₁₀H₈ClNO) C, H, N.

4-(1*H*-imidazol-1-yl)-2-methyl-8-quinolinol (12a). A solution of 4-chloro-2-methyl-8-quinolinol (**11**) (2.00 g, 10.3 mmol) and imidazole (3.52 g, 51.6 mmol) in 1,4-dioxane (20 mL) was refluxed for 6 h. After cooling, this mixture was partitioned between CHCl₃ and aqueous NaHCO₃. The organic layer was washed with water and brine, dried over MgSO₄, and evaporated in vacuo. The resulting residue was crystallized from Et₂O to afford **12a** (1.99 g, 85.5%) as colorless crystals: mp 192–196 °C; ¹H NMR (300 MHz, CDCl₃) δ 2.79 (s, 3H), 7.20–7.37 (m, 5H), 7.45 (dd, *J* = 8, 8 Hz, 1H), 7.86 (s, 1H), 7.61 (d, *J* = 8 Hz, 1H); MS (ESI) *m/z* 224 (M – 1). Anal. (C₁₃H₁₁N₃O) C, H, N.

Compounds **12b** and **12c** were prepared following the procedure described above for **12a**.

4-(Dimethylamino)-2-methyl-8-quinolinol (12d). A solution of 4-chloro-2-methyl-8-quinolinol (**11**) (3.50 g, 18.1 mmol) in DMF (5 mL) was refluxed for 16 h. After cooling, the reaction mixture was evaporated in vacuo and the resulting residue was washed with acetone and collected by vacuum filtration. The residue was partitioned between CHCl₃ and aqueous NaHCO₃. The organic layer was washed with water and brine, dried over MgSO₄, and evaporated in vacuo. The resulting residue was crystallized from hexane to afford **12d** (2.53 g, 69.2%) as colorless crystals: mp 192–196 °C; ¹H NMR (300 MHz, CDCl₃) δ 2.60 (s, 3H), 3.03 (s, 6H), 6.62 (s, 1H), 7.03 (d, *J* = 8 Hz, 1H), 7.25 (dd, *J* = 8, 8 Hz, 1H), 7.46 (d, *J* = 8 Hz, 1H); MS (ESI) *m/z* 203 (M + 1). Anal. (C₁₂H₁₄N₂O) C, H, N.

***N*-Methyl-4-((1*E*)-3-oxo-3-([2-oxo-2-(2,4-trimethyl-3-[[2-methyl-4-phenyl-8-quinolinyl]oxy]methyl)anilino]ethyl)amino)-1-propenyl)benzamide (14)**. To a mixture of **13b**²⁶ (165 mg, 0.386 mmol) and 2-methyl-4-phenyl-8-quinolinol (**6**) (99.8 mg, 0.424 mmol) in dry DMF (1.5 mL) were added K₂CO₃ (160 mg, 1.16 mmol) and tetrabutylammonium iodide (10 mg) at ambient temperature, and the mixture was stirred at the same temperature for 18 h. The reaction mixture was poured into saturated aqueous NaHCO₃ and extracted with EtOAc twice. The extracts were washed with brine. The water layer was extracted with CHCl₃. The organic layer was combined, dried over MgSO₄, and evaporated in vacuo. The residue was purified by flash silica gel chromatography (EtOAc/MeOH, 9:1) to afford **14** (181 mg, 74.9%) as a colorless amorphous solid: ¹H NMR (300 MHz, CDCl₃) δ 2.39 (s, 3H), 2.55 (s, 3H), 2.74 (s, 3H), 2.99 (d, *J* = 5 Hz, 3H), 3.26 (s, 3H), 3.64 (dd, *J* = 17, 4 Hz, 1H), 3.88 (dd, *J* = 17, 5 Hz, 1H), 5.37 (s, 2H), 6.25 (br q, *J* = 5 Hz, 1H), 6.50 (d, *J* = 15 Hz, 1H), 6.73 (br t, *J* = 5 Hz, 1H), 7.07 (d, *J* = 8 Hz, 1H), 7.16 (d, *J* = 8 Hz, 1H), 7.20–7.30 (m, 3H), 7.38 (dd, *J* = 8, 8 Hz, 1H), 7.44–7.60 (m, 8H), 7.74 (d, *J* = 8 Hz, 1H); MS (ESI) *m/z* 627 (M + 1). Anal. (C₃₉H₃₈N₄O₄) C, H, N.

4-[(1*E*)-3-((2-[2,4-Dichloro-3-([4-(1*H*-imidazol-1-yl)-2-methyl-8-quinolinyl]oxy)methyl)methyl)anilino]-2-oxoethyl)amino]-3-oxo-1-propenyl]-*N*-methylbenzamide (15a). To a mixture of **13a**²⁶ (52.4 mg, 0.102 mmol) and 4-(1*H*-imidazol-1-yl)-2-methyl-8-quinolinol (**12a**) (23.0 mg, 0.102 mmol) in dry DMF (0.5 mL) was added K₂CO₃ (42.3 mg, 0.306 mmol) at ambient temperature, and the mixture was stirred at the same temperature for 3 h. The reaction mixture was poured into water and extracted with EtOAc. The extracts were washed with brine, dried over MgSO₄, and evaporated in vacuo. The residue was purified by preparative thin-layer chromatography (CHCl₃/MeOH, 10:1) to afford **15a** (60 mg, 89.4%) as a colorless amorphous solid: ¹H NMR (300 MHz, CDCl₃) δ 2.79 (s, 3H), 3.02 (d, *J* = 5 Hz, 3H), 3.29 (s, 3H), 3.67 (dd, *J* = 17, 4 Hz, 1H), 3.93 (dd, *J* = 17, 5 Hz, 1H), 5.64 (d, *J* = 10 Hz, 1H), 5.69 (d, *J* = 10 Hz, 1H), 6.20 (br d, *J* = 5 Hz, 1H), 6.52 (d, *J* = 15 Hz, 1H), 6.68 (br t, *J* = 5 Hz, 1H), 7.30–7.61 (m, 10H), 7.75 (br d, *J* = 7.5 Hz, 2H), 7.83 (s, 1H); MS (ESI) *m/z* 657 (M + 1). Anal. (C₃₄H₃₀Cl₂N₆O₄) C, H, N.

Compounds **15b,c** and **49a** were prepared following the procedure described above for **15a**.

***N*-Methyl-4-((1*E*)-3-oxo-3-([2-oxo-2-(2,4-trimethyl-3-[[2-methyl-4-phenyl-8-quinolinyl]oxy]methyl)anilino]ethyl)amino)-1-propenyl)benzamide Hydrochloride (16)**. To a solution of **14** (160 mg, 0.255 mmol) in MeOH (2 mL) was added 10% HCl in MeOH (2 mL) at ambient temperature. The reaction mixture was stirred at the same temperature for 10 min. The solution was evaporated in vacuo and the residue was washed with EtOAc to afford **16** (139 mg, 82.1%) as a yellow amorphous solid: ¹H NMR (300 MHz, CDCl₃/CD₃OD) δ 2.32 (s, 3H), 2.50 (s, 3H), 2.96 (s, 3H), 3.12 (s, 3H), 3.29 (s, 3H), 3.80 (d, *J* = 17 Hz, 1H), 3.87 (d, *J* = 17 Hz, 1H), 5.42 (d, *J* = 9 Hz, 1H), 5.55 (d, *J* = 9 Hz, 1H), 6.64 (d, *J* = 15 Hz, 1H), 7.33 (s, 1H), 7.40–7.88 (m, 15H). Anal. (C₃₉H₃₈N₄O₄·iHCl) C, H, N.

Compounds **17a–c**, **23a–c**, **38**, **40**, **48ab**, **50a**, and **50b** were prepared following the procedure described above for **16**.

4-[(1*E*)-3-((2-[3-((*tert*-Butyl(diphenyl)silyloxy)methyl)-2,4-dichloromethyl)anilino]-2-oxoethyl)amino)-3-oxo-1-propenyl]-*N,N*-dimethylbenzamide (19). To a solution of **18**²⁶ (2.10 g, 4.19 mmol) in dry DMF (20 mL) were added (*E*)-4-(*N,N*-dimethylcarbamoyl)cinnamic acid (1.01 g, 4.61 mmol), 1-ethoxy-3-[3-(dimethylamino)propyl]carbodiimide hydrochloride (WSCD-HCl; 963 mg, 5.02 mmol), and 1-hydroxybenzotriazole (HOBt; 792 mg, 5.86 mmol) at ambient temperature. After 3 h, this mixture was partitioned between EtOAc and water. The organic layer was washed with saturated aqueous NaHCO₃, water, and brine, dried over MgSO₄, and evaporated in vacuo. The residue was purified by flash silica gel column chromatography (CHCl₃/MeOH, 50:1) to afford **19** (2.94 g, 99.9%) as a colorless amorphous solid: ¹H NMR (300 MHz, CDCl₃) δ 1.05 (s, 9H), 2.98 (br s, 3H), 3.10 (br s, 3H), 3.22 (s, 3H), 3.56 (dd, *J* = 17, 4 Hz, 1H), 3.94 (dd, *J* = 17, 5 Hz, 1H), 4.91 (d, *J* = 10 Hz, 1H), 4.97 (d, *J* = 10 Hz, 1H), 6.49 (d, *J* = 15 Hz, 1H), 6.60 (br s, 1H), 7.22 (d, *J* = 8 Hz, 1H), 7.34–7.60 (m, 12H), 7.69–7.78 (m, 4H); MS (ESI) *m/z* 702 (M + 1). Anal. (C₃₈H₄₁Cl₂N₃O₄Si) C, H, N.

Compounds **22a**, **37**, **45a,b**, and **49b** were prepared following the procedure described above for **19**.

4-[(1*E*)-3-((2-[2,4-Dichloro-3-(hydroxymethyl)methyl)anilino]-2-oxoethyl)amino)-3-oxo-1-propenyl]-*N,N*-dimethylbenzamide (20). To a solution of **19** (3.0 g, 4.27 mmol) in THF (30 mL) was added 1 M tetrabutylammonium fluoride in THF (6.4 mL) at ambient temperature. After 1 h, the mixture was partitioned between CHCl₃ and water. The organic layer was washed with water and brine, dried over MgSO₄, and evaporated in vacuo. The residue was purified by flash silica gel column chromatography (CHCl₃/MeOH, 15:1) to afford **20** (1.95 g, 98.4%) as a colorless amorphous solid: ¹H NMR (300 MHz, CDCl₃) δ 2.99 (br s, 3H), 3.12 (br s, 3H), 3.26 (s, 3H), 3.66 (dd, *J* = 17, 4 Hz, 1H), 3.90 (dd, *J* = 17, 5 Hz, 1H), 5.02 (br s, 2H), 6.49 (d, *J* = 15 Hz, 1H), 6.64 (br s, 1H), 7.28 (d, *J* = 8 Hz, 1H), 7.39–7.62 (m, 6H); MS (ESI) *m/z* 464 (M + 1). Anal. (C₂₂H₂₃Cl₂N₃O₄) C, H, N.

Compounds **46a** and **46b** were prepared following the procedure described above for **20**.

2,6-Dichloro-3-(((2*E*)-3-4-[(dimethylamino)carbonyl]phenyl)-2-propenoyl)amino]acetyl(methyl)amino)benzyl Methanesulfonate (21). To a solution of **20** (300 mg, 0.646 mmol) and Et₃N (78.5 mg, 0.775 mmol) in dry CH₂Cl₂ (3 mL) was added dropwise methanesulfonyl chloride (81.4 mg, 0.711 mmol) in an ice/water bath under nitrogen. After 10 min, the reaction mixture was stirred at ambient temperature for 30 min. This mixture was partitioned between CHCl₃ and water. The organic layer was washed with water, saturated aqueous NaHCO₃ and brine, dried over MgSO₄, and evaporated in vacuo to afford **21** (330 mg, 94.2%) as a pale-yellow amorphous solid: ¹H NMR (300 MHz, CDCl₃) δ 2.98 (br s, 3H), 3.06–3.18 (m, 6H), 3.26 (s, 3H), 3.62 (dd, *J* = 17, 4 Hz, 1H), 3.92 (dd, *J* = 17, 5 Hz, 1H), 5.54 (br s, 2H), 6.49 (d, *J* = 15 Hz, 1H), 6.62 (br s, 1H), 7.35–7.44 (m, 3H), 7.48–7.61 (m, 4H); MS (ESI) *m/z* 542 (M + 1). Anal. (C₂₃H₂₅Cl₂N₃O₆S) C, H, N.

4-[(1*E*)-3-({2-[2,4-Dichloro(methyl)-3-({2-methyl-4-(1*H*-pyrazol-1-yl)-8-quinolinyl}oxy)methyl]anilino)-2-oxoethyl}amino)-3-oxo-1-propenyl]-*N,N*-dimethylbenzamide (**22b**). To a solution of **21** (101 mg, 0.186 mmol) and 2-methyl-4-(1*H*-pyrazol-1-yl)-8-quinolinol (**12b**) (42 mg, 0.186 mmol) in dry DMF (1 mL) was added K₂CO₃ (77.3 mg, 0.559 mmol) at ambient temperature, and the reaction mixture was stirred at the same temperature for 18 h. The mixture was poured into water and extracted with EtOAc. The organic layer was washed with water three times, dried over MgSO₄, and evaporated in vacuo. The residue was purified by preparative thin-layer chromatography (CHCl₃/MeOH, 10:1) to afford **22b** (110 mg, 87.8%) as a colorless amorphous solid: ¹H NMR (300 MHz, CDCl₃) δ 2.79 (s, 3H), 2.98 (br s, 3H), 3.11 (br s, 3H), 3.28 (s, 3H), 3.58 (dd, *J* = 17, 4 Hz, 1H), 3.92 (dd, *J* = 17, 5 Hz, 1H), 5.68 (s, 2H), 6.50 (d, *J* = 15 Hz, 1H), 6.58 (br s, 1H), 6.67 (br s, 1H), 7.32 (d, *J* = 8 Hz, 2H), 7.38–7.61 (m, 8H), 7.78 (br d, *J* = 8 Hz, 1H), 7.84 (br s, 1H); MS (ESI) *m/z* 671 (*M* + 1). Anal. (C₃₅H₃₂Cl₂N₆O₄) C, H, N.

The compound **22c** was prepared following the procedure described above for **22b**.

Methyl (2*E*)-3-[4-[(4-Pyridinylamino)carbonyl]phenyl]-2-propenoate (25a). To a suspension of 4-[(1*E*)-3-methoxy-3-oxo-1-propenyl]benzoic acid (**24**)²⁵ (400 mg, 1.94 mmol) in thionyl chloride (1.4 mL, 19.4 mmol) was added DMF (1 drop) at ambient temperature, and the mixture was refluxed for 20 min. The reaction mixture was evaporated in vacuo and azeotropically removed with toluene. The residue was dissolved in CH₂Cl₂ (10 mL). To this solution were added 4-aminopyridine (201 mg, 2.13 mmol) and Et₃N (588 mg, 5.82 mmol) in an ice/water bath, and the reaction mixture was stirred at the same temperature for 3 h. The reaction mixture was poured into water and extracted with a mixture of CHCl₃ and MeOH (5:1). The organic layer was washed with saturated aqueous NaHCO₃, water, and brine, dried over MgSO₄, and evaporated in vacuo. The residue was crystallized from EtOAc to afford **25a** (555 mg, 82.5%) as crystals: mp 209–211 °C; ¹H NMR (200 MHz, DMSO-*d*₆) δ 3.76 (s, 3H), 6.82 (d, *J* = 15 Hz, 1H), 7.69–7.83 (m, 3H), 7.92 (d, *J* = 9 Hz, 2H), 8.01 (d, *J* = 9 Hz, 2H), 8.50 (d, *J* = 7 Hz, 2H). Anal. (C₁₆H₁₄N₂O₃) C, H, N.

Methyl (2*E*)-3-[4-[(2-Pyridinylmethyl)amino]carbonyl]phenyl]-2-propenoate (25b). To a solution of **24** (1.00 g, 4.85 mmol), 2-(aminomethyl)pyridine (577 mg, 5.33 mmol), and HOBt (852 mg, 6.30 mmol) in dry DMF (20 mL) was added WSCD·HCl (1.12 g, 5.82 mmol) at ambient temperature under nitrogen. After 4 h of stirring, this mixture was partitioned between EtOAc and water. The organic layer was separated, washed with saturated aqueous NaHCO₃, water, and brine, dried over MgSO₄, and evaporated in vacuo. The residue was purified by flash silica gel column chromatography (CH₂Cl₂/MeOH, 30:1) to afford **25b** (1.15 g, 79.7%) as a colorless amorphous solid: ¹H NMR (200 MHz, CDCl₃) δ 3.82 (s, 3H), 4.78 (d, *J* = 5 Hz, 1H), 6.50 (d, *J* = 15 Hz, 1H), 7.22 (dd, *J* = 9, 6 Hz, 1H), 7.32 (d, *J* = 9 Hz, 1H), 7.56–7.76 (m, 5H), 7.90 (d, *J* = 9 Hz, 2H), 8.58 (d, *J* = 6 Hz, 1H). Anal. (C₁₇H₁₆N₂O₃) C, H, N.

Ethyl (2*E*)-3-[4-(Isonicotinoylamino)phenyl]-2-propenoate (28). To a solution of ethyl (2*E*)-3-(4-aminophenyl)-2-propenoate (**27**)²⁵ (2.00 g, 10.46 mmol) in CH₂Cl₂ (30 mL) were added Et₃N (5.83 mL, 41.84 mmol) and isonicotinoyl chloride hydrochloride (2.23 g, 12.55 mmol) in an ice/water bath under nitrogen. The mixture was stirred at the same temperature for 30 min and stirred at ambient temperature for 3 h. The reaction mixture was washed with water, saturated aqueous NaHCO₃, and brine, dried over MgSO₄, and evaporated in vacuo. The residue was washed with EtOAc to afford **28** (2.00 g, 66.0%) as a colorless amorphous solid: mp 179–188 °C; ¹H NMR (200 MHz, CDCl₃) δ 1.34 (t, *J* = 7.5 Hz, 3H), 4.26 (q, *J* = 7.5 Hz, 2H), 6.40 (d, *J* = 16 Hz, 1H), 7.52 (d, *J* = 9 Hz, 2H), 7.57 (d, *J* = 16 Hz, 1H), 7.65–7.78 (m, 4H), 8.19 (br s, 1H), 8.31 (dd, *J* = 6, 1 Hz, 2H). Anal. (C₁₇H₁₆N₂O₃) C, H, N.

(2*E*)-3-[4-[(4-Pyridinylamino)carbonyl]phenyl]-2-propenoic Acid (26a). A suspension of **25a** (535 mg, 1.54 mmol)

in MeOH (5.4 mL) containing 1 N NaOH (1.7 mL) was heated at 60 °C for 2 h. Upon cooling, the reaction mixture was adjusted to pH 5 with 1 N HCl and diluted with water. The solid that precipitated was collected by vacuum filtration and washed with water to afford **26a** (401 mg, 78.2%) as crystals: mp >250 °C; ¹H NMR (200 MHz, DMSO-*d*₆) δ 6.69 (d, *J* = 16 Hz, 1H), 7.52–8.08 (m, 7H), 8.49 (d, *J* = 6 Hz, 2H). Anal. (C₁₅H₁₂N₂O₃) C, H, N.

Compounds **26b** and **29** were prepared following the procedure described above for **26a**.

3-Nitro-*N*-(4-pyridinyl)benzamide (31). To a mixture of 4-aminopyridine (1.83 g, 19.4 mmol) and Et₃N (2.45 g, 24.2 mmol) in CH₂Cl₂ (25 mL) was added a solution of 3-nitrobenzoyl chloride (**30**) (3.00 g, 16.2 mmol) in CH₂Cl₂ (5 mL) in an ice/water bath under nitrogen. The reaction mixture was stirred at the same temperature for 10 min and stirred at ambient temperature for 2 h. The precipitate was collected by vacuum filtration and washed with water and MeOH to afford **31** (3.42 g, 87.0%) as a solid: mp >250 °C; ¹H NMR (200 MHz, DMSO-*d*₆) δ 7.80 (d, *J* = 6 Hz, 2H), 7.89 (dd, *J* = 7, 7 Hz, 1H), 8.38–8.58 (m, 4H), 8.80 (t, *J* = 1 Hz, 1H). Anal. (C₁₂H₉N₃O₃) C, H, N.

3-Amino-*N*-(4-pyridinyl)benzamide (32). A mixture of **31** (1.09 g, 4.49 mmol) and 10% palladium on carbon (109 mg) in a mixture of MeOH (10 mL) and 1,4-dioxane (20 mL) was hydrogenated at ambient temperature. After completion of the reaction, the catalyst in the reaction mixture was removed by filtration. The solvent was evaporated in vacuo. The resulting residue was crystallized from EtOAc to afford **32** (901 mg, 94.2%) as pale-yellow crystals: mp 232–234 °C; ¹H NMR (200 MHz, DMSO-*d*₆) δ 5.39 (br s, 2H), 6.79 (br d, *J* = 8 Hz, 1H), 7.02–7.11 (m, 2H), 7.19 (dd, *J* = 8, 8 Hz, 1H), 7.78 (d, *J* = 7 Hz, 2H), 8.46 (d, *J* = 7 Hz, 2H). Anal. (C₁₂H₁₁N₃O) C, H, N.

Phenyl 3-[(4-Pyridinylamino)carbonyl]phenylcarbamate (33). To a solution of **32** (295 mg, 1.38 mmol) and 1 N NaOH (2.76 mL) in 1,4-dioxane (3 mL) was added phenyl chloroformate (260 mg, 1.66 mmol) in an ice/water bath. The reaction mixture was stirred for 30 min at the same temperature and poured into a mixture of water and CHCl₃. The precipitate was collected by vacuum filtration to afford **33** (460 mg, 99.7%) as a solid: mp 186–188 °C; ¹H NMR (300 MHz, DMSO-*d*₆) δ 6.75 (d, *J* = 6 Hz, 2H), 7.12 (dd, *J* = 7, 7 Hz, 1H), 7.20–7.30 (m, 2H), 7.35–7.50 (m, 2H), 7.55 (dd, *J* = 7, 7 Hz, 1H), 7.77 (d, *J* = 8 Hz, 2H), 8.16 (s, 1H), 8.30 (d, *J* = 6 Hz, 2H), 8.75 (d, *J* = 6 Hz, 2H). Anal. (C₁₉H₁₅N₃O₃) C, H, N.

***N*-[2,4-Dichloro-3-({4-(1*H*-imidazol-1-yl)-2-methyl-8-quinolinyl}oxy)methyl]phenyl]-2-(1,3-dioxo-1,3-dihydro-2*H*-isoindol-2-yl)-*N*-methylacetamide (35a)**. **Step 1**. To a solution of **34** (1.95 g, 4.96 mmol) and Et₃N (753 mg, 7.44 mmol) in dry CH₂Cl₂ (20 mL) was added dropwise methanesulfonyl chloride (625 mg, 5.46 mmol) in an ice/water bath under nitrogen. After 30 min, the reaction mixture was washed with water, saturated aqueous NaHCO₃, and brine. The organic layer was dried over MgSO₄ and evaporated in vacuo to afford the mesylate intermediate (2.35 g, ~100%) as a pale-yellow oil.

Step 2. To a solution of the crude mesylate intermediate (2.35 g, 4.99 mmol), tetrabutylammonium iodide (123 mg, 0.333 mmol), and 4 Å molecular sieves (340 mg) in dry DMF (38 mL) were added 4-(1*H*-imidazol-1-yl)-2-methyl-8-quinolinol (**12a**) (750 mg, 3.33 mmol) and K₂CO₃ (2.30 g, 16.6 mmol) in an ice/water bath, and the mixture was stirred at ambient temperature for 18 h. The reaction mixture was poured into water and extracted with CHCl₃. The organic layer was washed with water and brine, dried over MgSO₄, and evaporated in vacuo. The resulting residue was crystallized from EtOAc to afford **35a** (1.92 g, 96.0%) as pale-yellow crystals: mp 211–213 °C; ¹H NMR (300 MHz, CDCl₃) δ 2.81 (s, 3H), 3.25 (s, 3H), 4.09 (s, 2H), 5.70 (d, *J* = 10 Hz, 1H), 5.77 (d, *J* = 10 Hz, 1H), 7.24–7.64 (m, 8H), 7.69–7.78 (m, 2H), 7.81–7.90 (m, 3H); MS (ESI) *m/z* 600 (*M* + 1). Anal. (C₃₁H₂₃Cl₂N₅O₄) C, H, N.

Compounds **35b**, **47a**, and **47b** were prepared following the procedure described above for **35a**.

2-Amino-*N*-[2,4-dichloro-3-({[4-(1*H*-imidazol-1-yl)-2-methyl-8-quinolinyl]oxy}methyl)phenyl]-*N*-methylacetamide (36a). To a suspension of **35a** (1.91 g, 3.18 mmol) in EtOH (19 mL) was added hydrazine monohydrate (318 mg, 6.38 mmol) at ambient temperature, and the mixture was refluxed for 1 h. After the reaction mixture was cooled, the precipitates were filtered off. The filtrate was evaporated in vacuo, and to the residue was added CHCl₃ (20 mL). The precipitates were filtered off. The filtrate was evaporated in vacuo and the solid was washed with IPE to afford **36a** (1.50 g, 100%) as a pale-yellow amorphous solid: ¹H NMR (300 MHz, CDCl₃) δ 2.70 (br s, 3H), 2.92–3.12 (m, 2H), 3.24 (br s, 3H), 5.68 (br s, 2H), 7.18–7.55 (m, 8H), 7.85 (br s, 1H); MS (ESI) *m/z* 470 (M + 1). Anal. (C₂₃H₂₁Cl₂N₅O₂) C, H, N.

Compound **36b** was prepared following the procedure described above for **36a**.

3-({[2-[2,4-Dichloro-3-({[4-(1*H*-imidazol-1-yl)-2-methyl-8-quinolinyl]oxy}methyl)methylanilino]-2-oxoethyl]-amino)carbonyl)amino-*N*-(4-pyridinyl)benzamide (39). A mixture of **36a** (60.0 mg, 0.128 mmol), phenyl 3-[(4-pyridinylamino)carbonyl]phenylcarbamate (**33**) (44.6 mg, 0.134 mmol), and Et₃N (25.8 mg, 0.255 mmol) in dry DMF (0.6 mL) was stirred at 80 °C for 2 h. After cooling to ambient temperature, the reaction mixture was poured into water and extracted with EtOAc. The organic layer was washed with water three times, dried over MgSO₄, and evaporated in vacuo. The residue was purified by preparative thin-layer chromatography (CHCl₃/MeOH, 10:1) to afford **39** (57.0 mg, 63.0%) as a pale-yellow amorphous solid: ¹H NMR (300 MHz, CDCl₃) δ 2.76 (s, 3H), 3.27 (s, 3H), 3.91–4.01 (m, 2H), 5.39 (br d, *J* = 10 Hz, 1H), 5.54 (br d, *J* = 10 Hz, 1H), 6.50 (br s, 1H), 6.90 (s, 1H), 7.04 (dd, *J* = 8, 8 Hz, 1H), 7.23–7.58 (m, 10H), 7.84 (s, 1H), 7.90 (br d, *J* = 7 Hz, 2H), 8.31 (br s, 1H), 8.52 (br d, *J* = 7 Hz, 2H), 9.64 (br s, 1H); MS (ESI) *m/z* 709 (M + 1). Anal. (C₃₆H₃₀Cl₂N₈O₄) C, H, N.

1-(3-({[*tert*-Butyl(diphenyl)silyl]oxy}methyl)-2,4-dichlorophenyl)-1*H*-pyrrole (42). A solution of 3-({[*tert*-butyl(diphenyl)silyl]oxy}methyl)-2,4-dichloroaniline (**41**)²⁶ (6.08 g, 14.1 mmol) and 2,5-dimethoxytetrahydrofuran (1.87 g, 14.1 mmol) in AcOH (15 mL) was heated at 90 °C for 1 h. The mixture was evaporated in vacuo, and the residue was purified by flash silica gel column chromatography (hexane/EtOAc, 19:1) to afford **42** (5.82 g, 85.9%) as a pale-yellow oil: ¹H NMR (300 MHz, CDCl₃) δ 1.06 (s, 9H), 4.98 (s, 2H), 6.32 (d, *J* = 4 Hz, 2H), 6.83 (d, *J* = 4 Hz, 2H), 7.22 (d, *J* = 8 Hz, 1H), 7.32–7.48 (m, 7H), 7.74 (d, *J* = 8 Hz, 4H). Anal. (C₂₇H₂₇Cl₂NOSi) C, H, N.

1-[3-({[*tert*-Butyl(diphenyl)silyl]oxy}methyl)-2,4-dichlorophenyl]-1*H*-pyrrole-2-carbonitrile (43). To a solution of **42** (1.201 g, 2.50 mmol) in dry CH₂Cl₂ (12 mL) was added dropwise a solution of chlorosulfonyl isocyanate (455 mg, 3.22 mmol) in dry CH₂Cl₂ (2.8 mL) in a dry ice/CCl₄ bath below –20 °C under nitrogen. The reaction mixture was stirred in a dry ice/CCl₄ bath for 30 min and then at ambient temperature for 1 h. The mixture was cooled to –20 °C and treated with dry DMF (0.4 mL, 5.17 mmol). The reaction mixture was stirred at the same temperature for 30 min and then at ambient temperature for 1 h. To the mixture was added 4 N HCl (15 mL) in an ice/water bath, and the mixture was stirred for 30 min at that temperature. The organic layer was separated, washed with brine and saturated aqueous NaHCO₃, dried over MgSO₄, and evaporated in vacuo. The residue was purified by flash silica gel column chromatography (hexane/EtOAc, 9:1) to afford **43** (930 mg, 73.6%) as a pale-yellow oil: ¹H NMR (300 MHz, CDCl₃) δ 1.07 (s, 9H), 4.98 (s, 2H), 6.38 (t, *J* = 4 Hz, 1H), 6.93 (d, *J* = 4 Hz, 1H), 6.98 (d, *J* = 4 Hz, 1H), 7.31 (d, *J* = 8 Hz, 1H), 7.33–7.48 (m, 7H), 7.68–7.74 (m, 4H). Anal. (C₂₈H₂₆Cl₂N₂O₂Si) C, H, N.

1-[3-({[*tert*-Butyl(diphenyl)silyl]oxy}methyl)-2,4-dichlorophenyl]-1*H*-pyrrol-2-yl)methylamine (44). To a solution of **43** (820 mg, 1.62 mmol) in dry THF (16 mL) was added portionwise lithium aluminum hydride (74 mg, 1.95 mmol) at ambient temperature under nitrogen. The reaction mixture was stirred at the same temperature for 1 h. To the

mixture was added water (2 mL) dropwise in an ice/water bath. The precipitate was removed by vacuum filtration through Celite, which was then washed with EtOAc. The filtrate and washings were combined, and the organic layer was separated, dried over MgSO₄, and evaporated in vacuo. The residue was purified by flash silica gel column chromatography (CHCl₃/MeOH, 9:1) to afford **44** (414 mg, 50.2%) as a pale-yellow oil: ¹H NMR (300 MHz, CDCl₃) δ 1.06 (s, 9H), 3.52 (d, *J* = 15 Hz, 1H), 3.63 (d, *J* = 15 Hz, 1H), 4.97 (s, 2H), 6.30–6.19 (m, 2H), 6.63 (d, *J* = 4 Hz, 1H), 7.30 (d, *J* = 8 Hz, 1H), 7.34–7.48 (m, 7H), 7.68–7.79 (m, 4H). Anal. (C₂₈H₃₀Cl₂N₂O₂Si) C, H, N.

Biological Methods. Receptor Binding: Guinea Pig Ileum. The specific binding of [³H]BK (a high-affinity B₂ ligand) was assayed according to the method previously described⁴⁷ with minor modifications. Male Hartley guinea pigs (from Charles River Japan, Inc.) were killed by exsanguination under anesthesia. The ilea were removed and homogenized in ice-cooled buffer (50 mM sodium (trimethylamino)ethanesulfonate (TES) and 1 mM 1,10-phenanthroline, pH 6.8) with a Polytron. The homogenate was centrifuged to remove cellular debris (1000g, 20 min, 4 °C), and the supernatant was centrifuged (100000g, 60 min, 4 °C). The pellet was then resuspended in ice-cooled binding buffer (50 mM TES, 1 mM 1,10-phenanthroline, 140 μg/mL bacitracin, 1 mM dithiothreitol, 1 μM captopril, and 0.1% bovine serum albumin (BSA), pH 6.8) and was stored at –80 °C until use.

In the binding assay, the membranes (0.2 mg of protein/mL) were incubated with 0.06 nM of [³H]BK and varying concentrations of test compounds or unlabeled BK at room temperature for 60 min. Receptor-bound [³H]BK was harvested by filtration through Whatman GF/B glass fiber filters under reduced pressure, and the filter was washed five times with 300 μL of ice-cooled buffer (50 mM Tris-HCl). The radioactivity retained on the washed filter was measured with a liquid scintillation counter. Specific binding was calculated by subtracting the nonspecific binding (determined in the presence of 1 μM unlabeled BK) from total binding.

Cloned Human B₂ Receptors Expressed in CHO cells. CHO (dhfr⁻) cells that were transfected with, and stably expressed the human B₂ receptor, have been described previously.²⁹ Cells were maintained in a α -minimum essential medium supplemented with penicillin (100 μg/mL), streptomycin (100 μg/mL), and 10% fetal bovine serum. The cells were seeded in 48-well tissue culture plates at a density of 3.0 × 10⁴ cells/well and cultured for 1 day. The cells were washed three times with phosphate-buffered saline containing 0.1% BSA and incubated with 1.0 nM of [³H]BK and test compounds for 2 h at 4 °C in 0.25 mL of binding buffer III (20 mM HEPES, 125 mM *N*-methyl-D-glucamine, 5.0 mM KCl, 1.8 mM CaCl₂, 0.8 mM MgSO₄, 0.05 mM bacitracin, 5 μM enalaprilat, and 0.1% BSA, pH 7.2). All experiments were carried out three times. Nonspecific binding was determined in the presence of 1 μM unlabeled BK. At the end of the incubation, the buffer was aspirated, and the cells were washed twice with ice-cooled phosphate-buffered saline containing 0.1% BSA. The specific binding was calculated by subtracting the nonspecific binding, determined in the presence of 1 μM unlabeled BK, from the total binding. Bound radioactivity was determined by solubilizing with 1% sodium dodecyl sulfate containing 0.05 N NaOH and quantified in a liquid scintillation counter.

BK-Induced Bronchoconstriction in Guinea Pigs. Male Hartley guinea pigs weighing 470–750 g (from Charles River Japan, Inc.) were fasted overnight and anesthetized by intraperitoneal injection of sodium pentobarbital (30 mg/kg). Then the trachea and jugular vein were cannulated. The animals were ventilated at a tidal volume of 10 mL/kg with a frequency of 60 breaths/min through the tracheal cannula. To suppress spontaneous respiration, alcuronium chloride (0.5 mg/kg) was administered intravenously through the jugular vein cannula. Then, propranolol (10 mg/kg) was also administered subcutaneously. After 10 min, BK (5 μg/kg, dissolved in saline with 0.1% BSA) was administered intravenously through the jugular vein cannula. Bronchoconstriction was measured by the modified Konzett and Rossler method⁴⁸ as the peak

increase of pulmonary insufflation pressure (PIP).⁴⁹ Each dose of the compound dissolved in a 5% (w/v) citric acid solution or vehicle was administered through the same cannula 25 min after the first BK administration. BK was administered again 5 min after the drug injection, and bronchoconstriction was measured in the same manner. A 0% response was determined as PIP before the administration of BK, and the 100% response was determined as the first BK-induced bronchoconstriction before drug administration. The percent response was calculated from the following formula: % response = $(\Delta\text{PIP}_{\text{after drug}}/\Delta\text{PIP}_{\text{before drug}}) \times 100$. The efficacy of the drug was expressed as % inhibition, which was calculated from the values of % responses of drug-treated and vehicle groups as follows: % inhibition = $[1 - (\% \text{ response}_{\text{drug}})/(\% \text{ response}_{\text{vehicle}})] \times 100$.

Quantitative Determination of 48a in Rat Plasma by LC/MS/MS. Male Lewis rats ($n = 5$) were used. Compound 48a was dissolved in 5% aqueous solution of citric acid and was injected into the femoral vein (3.2 mg/1 mL/kg). Blood samples were taken from the femoral artery at 5, 10, 15, 30, 60, and 120 min after dosing followed by centrifugation. Plasma samples were prepared on the basis of an MeOH extraction and were analyzed on an HPLC (Alliance 2690, Waters, Milford, MA). Detection was performed on a tandem MS (Quattro Ultima, Micromass, Manchester, U.K.) by multiple reaction monitoring (MRM) mode via positive electrospray ionization (ESI). The precursor ion was m/z 679 and the product ion was m/z 461 in the MRM mode. The limit of quantitation was 10 ng/mL for plasma.

Statistical Analysis. The results are expressed as the mean \pm SEM, and statistical significance between groups was analyzed by Student's t test. IC₅₀ value was obtained by using nonlinear curve-fitting methods with a computer program developed in house.

Acknowledgment. We are grateful to Dr. D. Barrett (Medicinal Chemistry Research Laboratories, Fujisawa Pharmaceutical Co. Ltd., Osaka) for his valuable suggestions.

Supporting Information Available: Physical data for 12b,c, 15b,c, 17a-c, 22a,c, 23a-c, 26b, 29, 35b, 36b, 37, 38, 40, 45a,b, 46a,b, 47a,b, 48a,b, 49a,b, 50a, and 50b. This material is available free of charge via the Internet at <http://pubs.acs.org>.

References

- Ward, P. E. Metabolism of Bradykinin and Bradykinin Analogs. In *Bradykinin Antagonists: Basic and Clinical Research*; Burch, R. M., Ed.; Marcel Dekker: New York, 1991; pp 147–170.
- Regoli, D.; Barabé J. Pharmacology of Bradykinin and Related Kinins. *Pharmacol. Rev.* **1980**, *32*, 1–46.
- Dray, A.; Perkins, M. Bradykinin and Inflammatory Pain. *Trends Neurosci.* **1993**, *16*, 99–104.
- McEachern, A. E.; Shelton, E. R.; Bhakta, S.; Obernolte, R.; Bach, C.; Zuppan, P.; Fujisaki, J.; Aldrich, R. W.; Jarnagin, K. Expression Cloning of a Rat B₂ Bradykinin Receptor. *Proc. Natl. Acad. Sci. U.S.A.* **1991**, *88*, 7724–7728.
- Bouthillier, J.; Deblois, D.; Marceau, F. Studies on the Induction of Pharmacological Responses to Des-Arg⁹-Bradykinin in Vitro and in Vivo. *Br. J. Pharmacol.* **1987**, *92*, 257–264.
- Pruneau, D.; Luccarini, J. M.; Robert, C.; Belichard, P. Induction of Kinin B₁ Receptor-Dependent Vasoconstriction Following Balloon Catheter Injury to the Rabbit Carotid Artery. *Br. J. Pharmacol.* **1994**, *111*, 1029–1034.
- Marceau, F. Kinin B₁ Receptors: A Review. *Immunopharmacology* **1995**, *30*, 1–26.
- Wirth, K.; Bickel, M.; Hropot, M.; Günzler, V.; Heitsch, K.; Ruppert, D.; Schölkens, B. A. The Bradykinin B₂ Receptor Antagonist Icatibant (Hoe 140) Corrects Avid Na⁺ Retention in Rats with CCl₄-Induced Liver Cirrhosis: Possible Role of Enhanced Microvascular Leakage. *Eur. J. Pharmacol.* **1997**, *337*, 45–53.
- Arai, Y.; Takanashi, H.; Kitagawa, H.; Wirth, K. J.; Okayasu, I. Effect of Icatibant, a Bradykinin B₂ Receptor Antagonist, on the Development of Experimental Ulcerative Colitis in Mice. *Dig. Dis. Sci.* **1999**, *44*, 845–851.
- Stewart, J. M.; Gera, L.; Chan, D. C.; Whalley, E. T.; Hanson, W. L.; Zuzack, J. S. Potent, Long-Acting Bradykinin Antagonists for a Wide Range of Applications. *Can. J. Physiol. Pharmacol.* **1997**, *75*, 719–724.
- Stewart, J. M.; Gera, L.; Chan, D. C. Dimers of Bradykinin and Substance P Antagonists as Potential Anti-Cancer Drugs. *Pept. Sci.* **1999**, *1*, 731–732.
- Lembeck, F.; Wirth, K.; Winkler, I.; Breipohl, G.; Henke, S.; Knolle, J. EP Patent 0 661 058, 1995.
- Björck, L.; Sjöbring, U.; Ben Nasr, A.; Olsen, A.; Herwald, H.; Müller-Esterl, W. WO Patent 97 44353, 1997.
- Wirth, K. J.; Fink, E.; Rudolphi, K.; Heitsch, H.; Deutschländer, N.; Gabriele Wiemer, G. Amyloid β -(1–40) Stimulates Cyclic GMP Production via Release of Kinins in Primary Cultured Endothelial Cells. *Eur. J. Pharmacol.* **1999**, *382*, 27–33.
- Vavrek, R. J.; Stewart, J. M. Competitive Antagonists of Bradykinin. *Peptides* **1985**, *6*, 161–164.
- Hock, F. J.; Wirth, K.; Albus, U.; Linz, W.; Gerhards, H. J.; Wiemer, G.; Henke, S.; Breipohl, G.; König, W.; Knolle, J.; Schölkens, B. A. Hoe 140 a New Potent and Long Acting Bradykinin-Antagonist: In Vitro Studies. *Br. J. Pharmacol.* **1991**, *102*, 769–773.
- Wirth, K.; Hock, F. J.; Albus, U.; Linz, W.; Alpermann, H. G.; Anagnostopoulos, H.; Henke, S.; Breipohl, G.; König, W.; Knolle, J.; Schölkens, B. A. Hoe 140 a New Potent and Long Acting Bradykinin-Antagonist: In Vivo Studies. *Br. J. Pharmacol.* **1991**, *102*, 774–777.
- Cheronis, J. C.; Whalley, E. T.; Nguyen, K. T.; Eubanks, S. R.; Allen, L. G.; Duggan, M. J.; Loy, S.; Bonham, K. A.; Blodgett, J. K. A New Class of Bradykinin Antagonists: Synthesis and in Vitro Activity of Bissuccinimidoalkane Peptide Dimers. *J. Med. Chem.* **1992**, *35*, 1563–1572.
- Kyle, D. J.; Martin, J. A.; Burch, R. M.; Carter, J. P.; Lu, S.; Meeker, S.; Prosser, J. C.; Sullivan, J. P.; Togo, J.; Noronha-Blob, L.; Sinsko, J. A.; Walters, R. F.; Whaley, L. W.; Hiner, R. N. Proving the Bradykinin Receptor: Mapping the Geometric Topography Using Ethers of Hydroxyproline in Novel Peptides. *J. Med. Chem.* **1991**, *34*, 2649–2653.
- Kyle, D. J. Structure-Based Drug Design: Progress toward the Discovery of the Elusive Bradykinin Receptor Antagonists. *Curr. Pharm. Des.* **1995**, *1*, 233–254.
- Salvino, J. M.; Seoane, P. R.; Douy, B. D.; Awad, M. M. A.; Dolle, R. E.; Houck, W. T.; Faunce, D. M.; Sawutz, D. G. Design of Potent Non-Peptide Competitive Antagonists of the Human Bradykinin B₂ Receptor. *J. Med. Chem.* **1993**, *36*, 2583–2584.
- Sawutz, D. G.; Salvino, J. M.; Dolle, R. E.; Casiano, F.; Ward, S. J.; Houck, W. T.; Faunce, D. M.; Douy, B. D.; Baizman, E.; Awad, M. M. A.; Marceau, F.; Seoane, P. R. The Nonpeptide WIN-64338 Is a Bradykinin B₂ Receptor Antagonist. *Proc. Natl. Acad. Sci. U.S.A.* **1994**, *91*, 4693–4697.
- Gobeil, F.; Pheng, L. H.; Badini, I.; Nguyen-Le, X. K.; Pizard, A.; Rizzi, A.; Blouin, D.; Regoli, D. Receptors for Kinins in the Human Isolated Umbilical Vein. *Br. J. Pharmacol.* **1996**, *118*, 289–294.
- Abe, Y.; Kayakiri, H.; Satoh, S.; Inoue, T.; Sawada, Y.; Imai, K.; Inamura, N.; Asano, M.; Hatori, C.; Katayama, A.; Oku, T.; Tanaka, H. A Novel Class of Orally Active Non-Peptide Bradykinin B₂ Receptor Antagonist. 1. Construction of the Basic Framework. *J. Med. Chem.* **1998**, *41*, 564–578.
- Abe, Y.; Kayakiri, H.; Satoh, S.; Inoue, T.; Sawada, Y.; Inamura, N.; Asano, M.; Hatori, C.; Sawai, H.; Oku, T.; Tanaka, H. A Novel Class of Orally Active Non-Peptide Bradykinin B₂ Receptor Antagonists. 2. Overcoming the Species Difference between Guinea Pig and Man. *J. Med. Chem.* **1998**, *41*, 4053–4061.
- Abe, Y.; Kayakiri, H.; Satoh, S.; Inoue, T.; Sawada, Y.; Inamura, N.; Asano, M.; Aramori, I.; Hatori, C.; Sawai, H.; Oku, T.; Tanaka, H. A Novel Class of Orally Active Non-Peptide Bradykinin B₂ Receptor Antagonists. 3. Discovering Bioisosteres of the Imidazo[1,2-*a*]pyridine Moiety. *J. Med. Chem.* **1998**, *41*, 4062–4079.
- Abe, Y.; Kayakiri, H.; Satoh, S.; Inoue, T.; Sawada, Y.; Inamura, N.; Asano, M.; Aramori, I.; Hatori, C.; Sawai, H.; Oku, T.; Tanaka, H. A Novel Class of Orally Active Non-Peptide Bradykinin B₂ Receptor Antagonists. 4. Discovery of Novel Frameworks Mimicking the Active Conformation. *J. Med. Chem.* **1998**, *41*, 4087–4098.
- Inamura, N.; Asano, M.; Hatori, C.; Sawai, H.; Hirosumi, J.; Fujiwara, T.; Kayakiri, H.; Satoh, S.; Abe, Y.; Inoue, T.; Sawada, Y.; Oku, T.; Nakahara, K. Pharmacological Characterization of a Novel, Orally Active, Nonpeptide Bradykinin B₂ Receptor Antagonist, FR167344. *Eur. J. Pharmacol.* **1997**, *333*, 79–86.
- Aramori, I.; Zenkoh, J.; Morikawa, N.; O'Donnell, N.; Asano, M.; Nakamura, K.; Iwami, M.; Kojo, H.; Notsu, Y. Novel Subtype-Selective Nonpeptide Bradykinin Receptor Antagonists FR167344 and FR173657. *Mol. Pharmacol.* **1997**, *51*, 171–176.
- Asano, M.; Inamura, N.; Hatori, C.; Sawai, H.; Fujiwara, T.; Katayama, A.; Kayakiri, H.; Satoh, S.; Abe, Y.; Inoue, T.; Sawada, Y.; Nakahara, K.; Oku, T.; Okuhara, M. The Identification of an Orally Active, Nonpeptide Bradykinin B₂ Receptor Antagonist, FR173657. *Br. J. Pharmacol.* **1997**, *120*, 617–624.

- (31) Charkravarty, S.; Mavunkel, B. J.; Goehring, R. R.; Kyle, D. J. Novel Bradykinin Receptor Antagonists from a Structure-Directed Non-Peptide Combinatorial Library. *Immunopharmacology* **1996**, *33*, 61–67.
- (32) Saleh, T. S. F.; Vianna, R. M. J.; Creczynski-Pasa, T. B.; Charkravarty, S.; Mavunkel, B. J.; Kyle, D. J.; Calixto, J. B. Oral Anti-inflammatory Actions of NPC 18884, A Novel Bradykinin B₂ Receptor Antagonist. *Eur. J. Pharmacol.* **1998**, *363*, 179–187.
- (33) De Campos, R. O. P.; Alves, R. V.; Ferreira, J.; Kyle, D. J.; Charkravarty, S.; Mavunkel, B. J.; Calixto, J. B. Oral Antinociception and Edema Inhibition Produced by NPC 18884, a Non-Peptidic Bradykinin B₂ Receptor Antagonist. *Naunyn-Schmiedeberg's Arch. Pharmacol.* **1999**, *360*, 278–286.
- (34) Pruneau, D.; Luccarini, J. M.; Fouchet, C.; Defrène, E.; Franck, R. M.; Loillier, B.; Duclos, H.; Robert, C.; Cremers, B.; Bélichard, P.; Paquet, J. L. LF 160335, a Novel Potent and Selective Nonpeptide Antagonist of the Human Bradykinin B₂ Receptor. *Br. J. Pharmacol.* **1998**, *125*, 365–372.
- (35) Pruneau, D.; Paquet, J. L.; Luccarini, J. M.; Defrène, E.; Fouchet, C.; Franck, R. M.; Loillier, B.; Robert, C.; Bélichard, P.; Duclos, H.; Cremers, B.; Dodey, P. Pharmacological Profile of LF 16-0687, a New Potent Non-Peptide Bradykinin B₂ Receptor Antagonist. *Immunopharmacology* **1999**, *43*, 187–194.
- (36) Burgess, G. M.; Perkins, M. N.; Rang, H. P.; Campbell, E. A.; Brown, M. C.; McIntyre, P.; Urban, L.; Dziadulewicz, E. K.; Ritchie, T. J.; Hallett, A.; Snell, C. R.; Wrigglesworth, R.; Lee, W.; Davis, C.; Phagoo, S. B.; Davis, A. J.; Phillips, E.; Drake, G. S.; Hughes, G. A.; Dunstan, A.; Bloomfield, G. C. Bradyzide, a Potent Non-Peptide B₂ Bradykinin Receptor Antagonist with Long-Lasting Oral Activity in Animal Models of Inflammatory Hyperalgesia. *Br. J. Pharmacol.* **2000**, *129*, 77–86.
- (37) Dziadulewicz, E. K.; Ritchie, T. J.; Hallett, A.; Snell, C. R.; Davies, J. W.; Wrigglesworth, R.; Dunstan, A. R.; Bloomfield, G. C.; Drake, G. S.; McIntyre, P.; Brown, M. C.; Burgess, G. M.; Lee, W.; Davis, C.; Yaqoob, M.; Phagoo, S. B.; Phillips, E.; Perkins, M. N.; Campbell, E. A.; Davis, A. J.; Rang, H. P. Nonpeptide Bradykinin B₂ Receptor Antagonists: Conversion of Rodent-Selective Bradyzide Analogues into Potent, Orally-Active Human Bradykinin B₂ Receptor Antagonists. *J. Med. Chem.* **2002**, *45*, 2160–2172.
- (38) Heitsch, H. Non-peptide Antagonists and Agonists of the Bradykinin B₂ Receptor. *Curr. Med. Chem.* **2002**, *9*, 913–928.
- (39) Youngman, M. A.; Carson, J. R.; Lee, J. S.; Dax, S. L.; Zhang, S.-P.; Colburn, R. W.; Stone, D. J.; Codd, E. E.; Jetter, M. C. Synthesis and Structure–Activity Relationships of Aroylpyrrole Alkylamide Bradykinin (B₂) Antagonists. *Bioorg. Med. Chem. Lett.* **2003**, *13*, 1341–1344.
- (40) SYBYL Molecular Modeling System, version 6.7; Tripos, Inc., St. Louis, MO, 63144–2913.
- (41) Clark, M.; Cramer, R. D., III.; Van Opdenbosch, N. Validation of the General-Purpose Tripos 5.2 Force Field. *J. Comput. Chem.* **1989**, *10*, 982–1012.
- (42) Stewart, J. J. P. MOPAC: A Semiempirical Molecular Orbital Program. *J. Comput.-Aided Mol. Des.* **1990**, *4*, 1–105.
- (43) Kayakiri, H.; Abe, Y.; Oku, T. Design and Synthesis of a Novel Class of Highly Potent, Selective and Orally Active Nonpeptide Bradykinin B₂ Receptor Antagonists. *Drugs Future* **1999**, *24*, 629–646.
- (44) Farmer, S. G.; Powell, S. J.; Wilkins, D. E.; Grahem, A. Cloning, Sequencing, and Functional Expression of a Guinea Pig Lung Bradykinin B₂ Receptor. *Eur. J. Pharmacology* **1998**, *346*, 291–298.
- (45) Paquet, J. L.; Luccarini, J. M.; Fouchet, C.; Defrène, E.; Loillier, B.; Robert, C.; Bélichard, P.; Cremers, B.; Pruneau, D. Pharmacological Characterization of the Bradykinin B₂ Receptor: Inter-Species Variability and Dissociation between Binding and Functional Responses. *Br. J. Pharmacol.* **1999**, *126*, 1083–1090.
- (46) Cramer, R. D., III.; Patterson, D. E.; Bunce, J. D. Comparative Molecular Field Analysis (CoMFA). 1. Effect of Shape on Binding of Steroids to Carrier Proteins. *J. Am. Chem. Soc.* **1988**, *110*, 5959–5967.
- (47) Manning, D. C.; Vavrek, R.; Stewart, J. M.; Snyder, S. H. Two Bradykinin Binding Sites with Picomolar Affinities. *J. Pharmacol. Exp. Ther.* **1986**, *237*, 504–512.
- (48) Konzett, H.; Rössler, R. Versuchsanordnung zu Untersuchungen an der Bronchialmuskulatur. *Naunyn-Schmiedeberg's Arch. Exp. Pathol. Pharmacol.* **1940**, *195*, 71–74.
- (49) Asano, M.; Inamura, N.; Nakahara, K.; Nagayoshi, A.; Isono, T.; Hamada, K.; Oku, T.; Notsu, Y.; Kohsaka, M.; Ono, T. A 5-Lipoxygenase Inhibitor, FR110302, Suppresses Airway Hyperresponsiveness and Lung Eosinophilia Induced by Sephadex Particles in Rats. *Agents Actions* **1992**, *36*, 215–221.

JM030159X